MODELING THE DISTINCT EFFECTS OF HIV PROTEASE INHIBITORS ON THE CONFORMATION AND MECHANISM OF MOUSE P-GLYCOPROTEIN

by

ED JOWELSON ABALLE BELOCURA
(Under the Direction of Arthur G. Roberts)

ABSTRACT

The P-glycoprotein (P-gp) protein pump is implicated in the efflux of a very significant number of drugs currently on the market. Since their creation, the efficacy of HIV protease inhibitor drugs have known to be significantly affected by P-gp efflux. This complicates the drawbacks of mainstream HIV drug treatment known as highly active antiretroviral treatment (HAART). HAART is already vulnerable to the development of HIV drug resistance, the sequestering of HIV into sanctuary sites, and overall poor oral drug bioavailability. Newer evidence suggests that in addition to being transported out of cells as P-gp substrates these drugs can also work as P-gp inhibitors, creating a more complicated and unique picture of how these drugs interact with P-gp. Four HIV protease inhibitors were selected for this study: saquinavir, ritonavir, indinavir, and lopinavir. The goal is to investigate the differences in their binding profiles with P-gp and to determine a model that can characterize these drugs' unique P-gp interactions.

INDEX WORDS: P-glycoprotein, ATPase kinetics, binding affinity, conformational change, efflux, ABC transporters, HIV protease inhibitor

MODELING THE DISTINCT EFFECTS OF HIV PROTEASE INHIBITORS ON THE CONFORMATION AND MECHANISM OF MOUSE P-GLYCOPROTEIN

By

ED JOWELSON ABALLE BELOCURA

B.S., University of Georgia, 2021

A Thesis Submitted to the Graduate Faculty of The University of Georgia in Partial Fulfillment of the Requirements for the Degree

MASTER OF SCIENCE

ATHENS, GEORGIA

2022

MODELING THE DISTINCT EFFECTS OF HIV PROTEASE INHIBITORS ON THE CONFORMATION AND MECHANISM OF MOUSE P-GLYCOPROTEIN

By

ED JOWELSON ABALLE BELOCURA

Major Professor:	Arthur Roberts
Committee:	Neil Grimsey Eugene Douglass

Electronic Version Approved:

Ron Walcott
Vice Provost for Graduate Education and Dean of the Graduate School
The University of Georgia
August 2022

DEDICATION

I would like to give a big shoutout to Julia Lopez and TJ Hasan, along with Amir, Khris, and Macy. This very short and yet oh-so long of a journey marked a very weird and transitionary point in my life. I was glad to share this past year with the 914 Cronies. To Julia, no one has ever believed in me more than you have. Thank you.

Big ups to my family. To my parents, you've never stopped pushing me to be a better person than I was yesterday. To my sister – my biggest inspiration. I believe in tomorrow partly because people like my sister, who tirelessly fight for the future, exist.

I would not be here without them.

I would like to thank Gershon Mensah and Amanda Kozarich for their immense support. My journey as a scientist was full of failure and doubt, but also joy and laughter. You guys were patient and you were kind. I can't ever thank you enough for that.

I would also like to dedicate this work to the countless live lost to HIV and to the millions who still struggle against this virus today. Writing a thesis on HIV and P-gp has been a far more intimate and emotional journey than I ever expected. Let's hope for and work towards a brighter future.

Finally, I would like to thank Dr. Audie for his incredible guidance. You've been a light and inspiration to all of us in lab. You've never failed to remind us to live our lives with pride and determination. At the end of the day, we are only human.

Table of Contents

List of Figures

Chapter 1

Introduction

1.1 HIV/AIDS

Disease Background

Four decades ago, the Centers for Disease Control (CDC) established and defined a new disease called acquired immunodeficiency syndrome (AIDS). In 1982, AIDS was an emerging mysterious disease with no known causes with an alarming death rate. By the end of the year, 771 reported cases and 618 deaths were recorded in the US alone. In the following years, the outbreak erupted into a global epidemic that would go on to infect an estimated current total of 79.3 million people. In the wake of the devastating effects of this rapidly spreading disease, the scientific community scrambled to identify the causative agent of AIDS. Working with a small number of clues and using blood samples from patients, two independent laboratories successfully isolated and identified a new strain of retrovirus that was implicated in the development of symptoms that were found in nearly all AIDS patients (Gallo et al., 1983) (Barré-Sinoussi et al., 1983). Today, we know of this virus as human immunodeficiency virus (HIV). Work on antiretroviral drugs immediately began and resulted in the fast-track approval for Zidovudine in 1987. This drug specifically targets reverse transcriptase, which is an enzyme crucial to retrovirus reproduction. While the arrival of the first antiretroviral therapies (ART) was a godsend for the HIV-positive population, drug resistant strains of the virus emerged. The medical community realized that

they would need to weaponize different treatment options simultaneously in order to continue the fight against HIV. Researchers continued to investigate other potential drug targets. In 1988 the HIV-1 protease enzyme was discovered, which cleaves the HIV polypeptide required to produce a mature viral genome during the final step of viral synthesis (Graves M C et al., 1988).

Development of HAART

In 1995, the FDA approved the first HIV protease inhibitor drug saquinavir. Marketed as Invirase, this drug ushered in a new era of HIV medicine by combining with other ART drugs to form highly active antiretroviral treatment (HAART). It was reported that a combination of multiple drugs in HAART treatment significantly reduced AIDS-related mortalities by 60-80% (Becker, 2018). The advent of HAART marked a shift towards multidrug treatments that targeted the various mechanisms through which HIV infection occurred. The first generation HIV protease inhibitor (PI) drugs were based on a peptidomimetic structure, in that they mimic the transition that forms between HIV protease and its peptide substrate (Ghosh et al., 2016). However, just like the earlier reverse transcriptase inhibitors, they still were still vulnerable to reduced efficacy due to mutation-based drug resistance. Scientists also began to understand that they were fighting two fronts in the war against HIV: the first was against viral drug resistance and the second was against our own internal physiological drug resistance caused by ABC transporters like P-glycoprotein.

A large 170 kDa transmembrane protein ubiquitously expressed throughout the human body, P-glycoprotein is understood to be a cellular defense mechanism against foreign substances. Sometimes known as multidrug resistance protein 1 (MDR1) and ABCB1, it acts by pumping these substances back out into the extracellular space, akin to a hydrophobic household vacuum cleaner. In the case of HIV PI drugs, it prevents them from accumulating to therapeutically effective concentrations. While later generation HIV PI drugs such as darunavir have proven far more resilient to HIV protease drug resistance, there still is no answer for the effects of MDR1 protein (Ghosh et al., 2016).

Most patients seeking HAART treatment today have multiple classes of anti-HIV drugs to choose from. These include HIV protease inhibitors (PI's), nucleoside reverse transcriptase inhibitors (NRTI's), non-nucleoside reverse transcriptase inhibitors (NNRTI's), nucleotide reverse transcriptase inhibitors (NtRTI's), HIV-fusion inhibitors, integrase inhibitors, and CC chemokine receptor type 5 antagonists (Tang & Shafer, 2012). PI's and NNRTI's are particularly more prone to drug-drug interactions due to their interactions with cytochrome P450 isozymes, which can be problematic since HAART usually requires the administration of least three complementary drugs. Since AIDS is commonly associated with other comorbidities that may require additional drug treatment, and with CYP3A4 genetic polymorphisms taken into consideration, planning around drug interactions can pose a very significant challenge for healthcare providers (Josephson, 2010). Ritonavir, a first-generation PI drug which was initially used for frontline treatment, is now used as a pharmacokinetic booster in HAART. Its well-documented inhibitory effect on CYP3A4 activity is used alongside other PI drugs to boost their bioavailability.

Progress in the research on HIV pathogenesis, along with advancements in biology and drug development have ushered in these antiviral therapies that have successfully slowed down the spread of AIDS and drastically cut down the AIDS-related mortality rate. What was once a mysterious and incurable fatal disease is now a chronic disease that is manageable with treatment. Today, HIV-positive patients who receive HAART treatment early enough are expected to have about the same life expectancy as HIV-negative people (Hayes, 2021). However, the fight against AIDS/HIV is still far from over. Every day, 4000 more people become newly infected with HIV. With infection rates starting to rise all over the world, it is estimated that 1.2 million people may be newly infected by 2025 – a figure much large than the initial expected initial estimate (*UNAIDS Global AIDS Update 2022*, 2022). Multidrug resistance transporters like P-gp stand in the way of achieving a cure through total viral eradication. As

we draw closer to 2030 – the year that the US hopes to end the HIV epidemic, the race is on to find new solutions to this ever-growing and continuously evolving problem.

1.2 HIV Protease

Structure of HIV Protease

HIV-1 protease is an aspartic protease, meaning its catalytic site is composed of aspartic acid residues that utilize an activated water molecule to catalyze peptide hydrolysis. Its overall structure is comprised of a symmetric homodimer, each half consisting of 99 amino acids. The Asp-25 residues from each monomer make up the active site, which sits right in the middle of the enzyme. The three most relevant sites on HIV protease's structure include the active site, the flexible flaps that can cover and expose it, and the dimer interface. Crystal structures have shown that the protease with no bound ligand exhibits the open conformation at the active site (Weber & Agniswamy, 2009). When a substrate is bound, the flaps cover the active site leading to a closed conformation which prevent the reactants from spilling out of the active site.

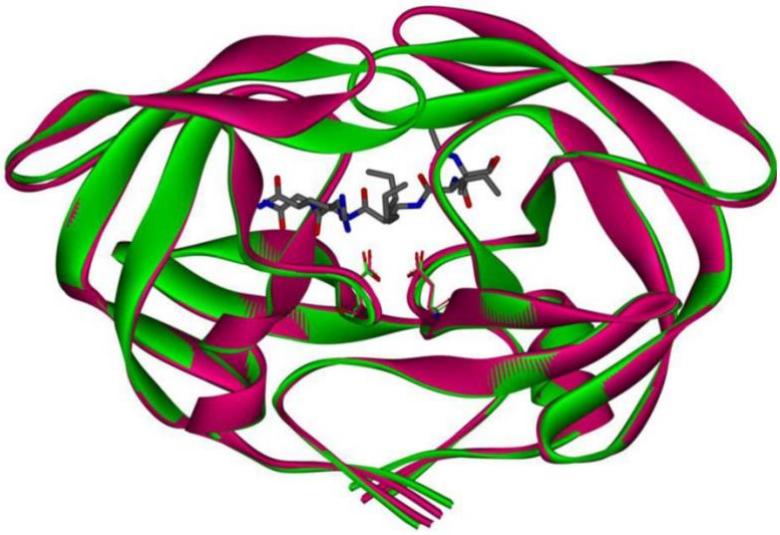

Figure 1 HIV protease in both the flap open (magenta, PDB: 2PCO)[61] and flap closed conformations (green, PDB: 2AOD)[62] shown as ribbons. Catalytic residues Asp25 and Asp25' of both enzymes are shown in sticks. Peptide inhibitor ace-Thr-Ile-Nle-r-Nle-Gln-Arg is shown in sticks, where r is the reduced peptide bond.

*Note: Figure and caption reprinted from Ghosh, A. K., Osswald, H. L., & Prato, G. (2016). Recent Progress in the Development of HIV-1 Protease Inhibitors for the Treatment of HIV/AIDS. *Journal of Medicinal Chemistry*, *59*(11), 5172–5208. https://doi.org/10.1021/acs.jmedchem.5b01697

Mechanisms for Drug Resistance

The molecular basis for drug resistance is largely caused by mutations in the HIV protease enzyme. The HIV-1 virus has a very high mutation rate. Mutations are picked up at an estimated one nucleotide mutation for every replication cycle (Tang & Shafer, 2012). It only takes a few mutations in key residues or areas on HIV protease to stop an inhibitor drug from binding. There are several factors that can contribute to this. Reverse transcriptase notoriously has very poor proofreading ability as it transcribes the viral RNA into DNA. This very high rate of mutation is compounded by the high rate of viral replication. Even for individuals who become infected with a single or few copies of HIV, it is estimated that about 10^{10} virion copies get produced each day (Tang & Shafer, 2012). The complexity of this picture is taken a step further when one considers the high recombination rates that can occur when different viral mutants invade the same host cell. All of these factors contribute to HIV's remarkable ability to continuously evolve drug resistance. As effective as these drugs are, over time mutants that confer better resistance against protease inhibitors will be selected and these drugs will become less effective against those mutants.

Mutations to the HIV protease structure can be classified in several different ways, depending on the literature. The simplest classification distinguishes primary and secondary mutations. Primary mutations occur in the residues that are actively involved in substrate binding. This would encompass everything within the active site. These types of mutations would result in reduced interactions between the enzyme and the protease inhibitor, attenuating the latter's anti-HIV effect. Secondary mutations could alter the stability of the dimer. These mutations also include changes to residues in the more

distal regions of the enzyme, which in turn could transmit changes to the binding site, where van der Waal's interactions and hydrogen-bonding are crucial to anchoring the substrate. (Ghosh et al., 2016).

Mechanism of HIV-1 Protease

During HIV infection, the virus invades T-helper cells by latching on to their external CD4 receptors. The entire virus and its contents are endocytosed into the host through membrane fusion. Reverse transcriptase creates DNA copies of the viral RNA using the host's own nucleotides, after which integrase incorporates the HIV DNA into the host cell's genome. This genome integration is the cause of lifelong infection and is part of why HIV is notoriously difficult to eradicate. Messenger RNA transcribed from the integrated viral DNA encode for various viral proteins, which are crucial to continuing the HIV life cycle. Using the host's ribosomes and cellular machinery, the viral DNA is translated into a long single polypeptide.

During the budding process, as the near-mature HIV particle is about to released from the host cell, HIV protease catalyzes the cleaving of the *Gag* and *Gag-Pol* polyproteins at various sites. This process produces the mature proteins required to continue on the HIV replication cycle. Blocking HIV protease from carrying out this function essentially blocks viral maturation (Weber & Agniswamy, 2009).

It is now understood that the two catalytic Asp-25 residues have significantly different pK_a values of ~3.5 ± 0.1 and ~6.0 ± 0.5. This seems to imply that the catalytic site is monoprotonated. (Kumar et al., 2020). A water molecule present inside the active site is activated by the non-protonated Asp residue and subsequently attacks the carbonyl of the substrate's peptide bond, forming a tetrahedral intermediate. This intermediate between the protease and the peptide is shown up close in Figure 2. This intermediate is held inside by the protease flaps in the closed conformation. The tetrahedral intermediate collapses to its separate products when the catalytic Asp transfers a proton to the N of the peptide bond, finalizing the cleavage of the polypeptide.

HIV protease inhibitors come into play as competitive inhibitors, directly binding to the protease's active site. Their structure mimics the tetrahedral transition state that is formed with the typical peptide substrate. As they occupy the protease's active site, the flaps are locked into the closed conformation. The conformation of the flaps is crucial to allowing the substrate and products to enter and leave the active site. With protease inhibitor drug bound to the active site, the further cleavage of HIV polyprotein is prevented.

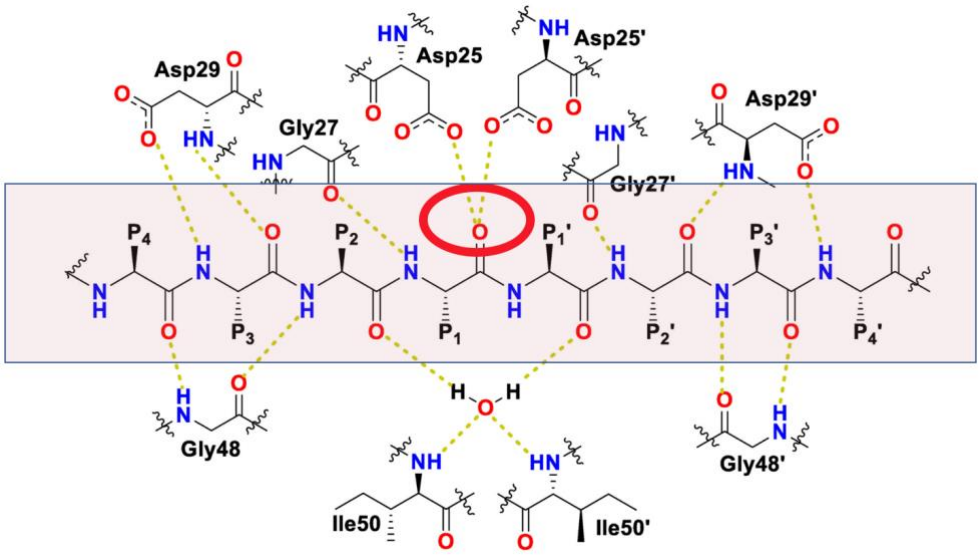

Figure 2 Interactions between the protease catalytic residues and the peptide substrate. The shaded area indicates the peptide. Yellow dotted lines show the stabilizing interactions between the two. Hydrolysis of the peptide is catalyzed by Asp25 and Asp25' on the carbonyl indicated by the red circle.

*Note: Figure adapted from Ghosh, A. K., Osswald, H. L., & Prato, G. (2016). Recent Progress in the Development of HIV-1 Protease Inhibitors for the Treatment of HIV/AIDS. *Journal of Medicinal Chemistry*, *59*(11), 5172–5208. https://doi.org/10.1021/acs.jmedchem.5b01697

Drawbacks of Current Treatments

Despite the plethora of HIV drugs that are currently out on the market, we are still far from achieving 100% viral eradication with mainstream HAART treatment. Eradication has been achieved in at least 3 extraordinary cases, but these involved experimental treatments of stem cell transplants from donors with double CCR5-delta-3 mutation (Highleyman, 2022). CCR5 is an endogenous co-receptor

involved in the mechanism by which HIV attacks T helper cells. Exceedingly rare as they are, these cases give hope that HIV total eradication is a concept that can work.

As for now, HAART regimens are capable of lowering a patient's viral load to essentially undetectable levels, but that comes at the cost of having to stay on the drug treatment for life. Although the HIV medications of today are generally well-tolerated, they still come with a lot of side effects, some of which can be severe. Some of the common PI drug side effects include profuse diarrhea, nausea, fatigue, along with a host of potentially more serious metabolic syndromes such as dyslipidemia and lipodystrophy/lipoautotrophy, and cardiovascular problems (Lv et al., 2015). Adhering to daily treatment schedules, while also having to manage whatever lifelong side effects can arise offers a very significant challenge for patients. HIV PI drugs typically have very low oral bioavailability. First generation PI's were designed to have a "peptide-like" structure, which makes them prone to being quickly metabolized. This resulted in higher and more frequent dosages needed to stay within the therapeutic windows. The emergence of drug-resistant HIV protease strains since HAART became widely available has also been very problematic. A study estimated that about 40-50% of patients that found initial success with HAART will eventually experience treatment failure due to evolved resistance (Ghosh et al., 2007).

Many these drugs are extensively metabolized by CYP450 enzymes, which can cause therapy failure resulting from suboptimal drug plasma concentrations. Other drugs some can also simultaneously inhibit CYP450 activity as they are metabolized, which can boost the pharmacological effect of other drugs that a patient may be taking (Eagling et al., 1997). Genetic polymorphisms of the CYP450 enzyme system can introduce unpredictability in how these drug-drug interactions can occur across different individuals. Besides P-gp, other ABC transporters such as MRP1 and BCRP can have significant contributions to drug efflux from cells.

One of the most significant roadblocks to achieving complete viral eradication with HIV PI drugs is the existence of sanctuary sites in the body. These are tissue reservoirs in which increased levels of P-

gp expression and efflux that limits the accumulation of HIV drugs within the tissue. The biggest example is the brain, protected by the blood-brain barrier (BBB) which boasts a high concentration of P-gp throughout the brain capillary endothelial cells (Robillard et al., 2014) (Agrawal et al., 2020). Other examples include the testis and ovaries, which are protected by their own P-gp rich endothelial barriers. Due to the decreased therapeutic effect of HIV PI drugs in these sanctuary sites, HIV accumulates in these tissues while it is inhibited throughout the rest of the body. The existence of sanctuary sites presents 3 major negatives to HIV treatment: 1) they impede the accumulation of therapeutic agents in specific parts of the body, preventing a complete cure, 2) they allow viral replication to continue for extended periods of time, therefore providing a haven for drug resistant mutants to continue evolving, and 3) there is evidence of disorders associated with physical areas of the body where these sanctuary sites occur. For example, up to 30-50% of HIV patients experience HIV associated neurocognitive disorders (HAND), which is linked to the inability of HAART drugs to cross the BBB (Omeragic et al., 2020). The severity of HAND is spread across a spectrum, which doesn't necessarily progress into the most severe disorders. This spectrum can range from asymptomatic impairment to minor neurocognitive disorder, which is accompanied by impaired mental faculties that affects everyday life. HIV-associated dementia is the most severe form of HAND. Up to 30-50% of HIV patients will experience some form of HAND, regardless of whether they are adherent to HAART or not. It has been observed that long-term exposure to HIV PI drugs can induce the up-regulation of P-gp expression, which decreases these drugs' already low ability to penetrate the blood-brain barrier (Zastre et al., 2009) (Perloff et al., 2001). As a result, extended therapy can become less effective over time.

1.3 P-gp and HIV Protease Inhibitors

There is an overwhelming amount of evidence from the past several decades that points the fact that many HIV PI drugs are both *in vitro* and *in vivo* transported by P-glycoprotein (Kim et al., 1998) (Washington et al., 2000) (Perloff et al., 2001) (Yamazaki et al., 2001) (Janneh et al., 2007). However,

there is more recent emerging evidence that seems to suggest these drugs are not anywhere near as efficient substrates as they were thought to be, with some of them exhibiting more inhibitory activity on P-gp (Bierman et al., 2010) (Cerveny et al., 2018) (Zolnerciks et al., 2011). Without a shadow of a doubt, there are strong interactions between this elusive transporter protein and the drugs investigated in this study. Many substances that do interact with P-gp exhibit either substrate-like behavior or inhibitor-like behavior. The idea that efflux and inhibition must be mutually exclusive can be ruled out, since there are known drugs and substances that exhibit both behaviors (Ledwitch et al., 2016) (Griffin et al., 2011). It has been proposed that drugs that exhibit both types of behavior may have multiple binding spots on P-gp, which could be either activating or inhibitory in effect (Calabrese, 2008). That case could be applied to HIV PI drugs.

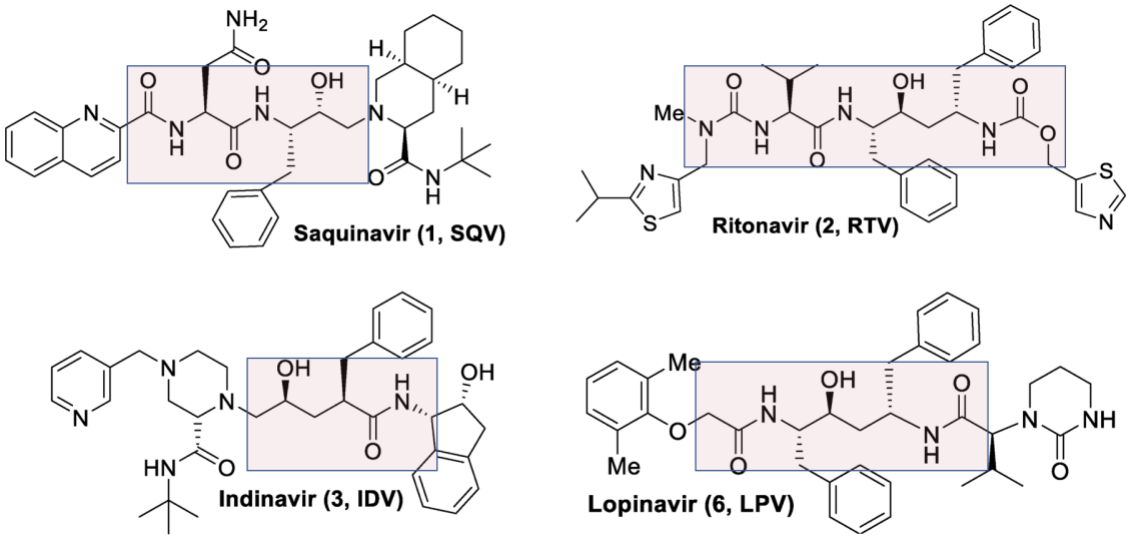

Figure 3 Structure of protease inhibitors used in this study. The shaded area represents the "peptide-like" area of the drug, as first-generation protease inhibitors were designed with this common philosophy in mind. The side groups are involved in various molecular interactions with protease residues, the strength of which may affect the efficacy of these drugs. Correspondingly, the variation in side groups are likely what is causing different behaviors in P-gp interactions.

Purpose

This research will investigate the differences between how four selected first generation HIV protease inhibitors – saquinavir, ritonavir, indinavir, and lopinavir – bind to mouse P-gp. The purpose is to determine a model for characterizing these drugs' unique interactions with this elusive transporter. There are many similarities in these drugs' structures, largely due to the peptide-like design philosophy of the first-generation HIV PI drugs. If a model or pattern of PI binding with mouse P-gp can be determined, hopefully this work can be a starting point to find similar models with human P-gp.

This research was accomplished through a series of methods. The first method involved measuring the drug-induced P-gp ATPase hydrolysis kinetics with each drug, to get an idea of the reaction kinetics for comparison. Two fluorescence spectroscopy methods were also used to probe the changes in P-gp's conformational states with different conditions of drug. Combined, these three data sets should be substantial enough to provide an understanding for HIV PI drug binding behavior with P-gp.

1.4 P-glycoprotein

ABC Transporter Family and Background on P-glycoprotein

The ATP-binding cassette (ABC) transporter family is one of the largest known protein families studied in biomedical science. This ancient family of proteins is found in virtually all living organisms, and has been studied in ancient prokaryotes to every modern eukaryotes (Vasiliou et al., 2009). The ABC superfamily includes P-glycoprotein (ABCB1), MRP1 (ABCC1), and BCRP (ABCG2). The discovery of Permeability-glycoprotein in 1975 sparked broad interest from many researchers in different areas of biomedicine (Hamdoun et al., 2021).

The ABC transporter is aptly named for the for adenosine triphosphate (ATP) molecule that is required to bind in order to transport its substrates. Contrary to how many familiar enzymes behave, these protein pumps have an incredibly broad selection of possible substrates. P-gp itself can recognize

and transport hundreds of different compounds, within a wide range of sizes from 330 to 4000 daltons. (Aller Stephen G. et al., 2009). It has been recognized that the majority of P-gp substrates are hydrophobic, can partition into the lipid bilayer, weakly basic, and many of them include aromatic rings (Aller Stephen G. et al., 2009) (Choi & Yu, 2014).

P-gp is currently understood as a defense mechanism against the accumulation of exogeneous compounds, toxic drugs and metabolites, ions, and peptides within living cells. Although it is ubiquitously expressed throughout the body it is concentrated in several tissues, for example on the luminal surface of the intestinal epithelia, on the blood-brain barrier, the placenta, the renal proximal tubule, and the hepatocyte bile canalicular membrane (Zolnerciks et al., 2011). These tissues are all involved, in some degree, to maintaining homeostatic processes. Their ability to regulate the ins and outs of many different compounds are critical to supporting that function. The overexpression of P-gp is widely associated with general resistance to therapeutic drugs, hence the alternative name “multidrug resistance protein 1” (MDR1) that P-gp is commonly known by (Jain et al., 2018).

Despite the wealth of research that has been published in the decades since its discovery, there still remain many unanswered questions about P-gp. What is universally agreed upon is that 1) P-gp efflux is an ATP-dependent process that is coupled with the binding and subsequent hydrolysis of ATP to drive the transport of a diverse range of substrates across the cell membrane, usually against a concentration gradient; 2) ATP allows for the switching of conformational states, between either an open conformation that faces inwards to the cytoplasm or a closed conformation that opens up towards the extracellular side; 3) P-gp efflux is unidirectional.

Much of the biomedical literature concerned with P-gp is based on either human cells engineered to overexpress P-gp or with mouse P-gp directly. The general structure of ABC transporters is relatively conserved across most species. With P-gp specifically, it was found that the amino acid sequence was highly conserved among human, rat, and mouse MDR1 samples. Mouse P-gp and human

ABCB1 are 87% identical in sequence (Jain et al., 2018). Due to the difficulties associated with expressing human MDR1 in *Pichia pastoris* yeast, this project focuses solely on mouse P-gp. For the purpose of this study, they are similar enough to postulate what could potentially happen in human P-gp. Once a model is determined with using mouse P-gp, further work can be done to see if the model is translatable in human P-gp.

Structure of P-glycoprotein

Most of the structural information that we have from P-gp is obtained from X-ray crystallography studies, cryo EM studies, and FRET analyses (Aller Stephen G. et al., 2009) (Frank et al., 2016) (Kodan et al., 2021). The structure of mouse P-gp is divided into two symmetrical halves, each with a portion that extends into the extracellular space and a portion that extends into the cytoplasm. The symmetrical opposing halves comprise six transmembrane helical segments and a nucleotide binding site, where ATP can bind. Considering the overall structure, P-gp can be thought of as consisting of four main functional domains: 2 transmembrane domains (TMD's) and 2 nucleotide binding domains (NBD's). Studies to understand which residues were responsible for substrate binding found that they were distributed all throughout the transmembrane helices (Esser et al., 2016). In other words, the hydrophobic TMD's largely determine what the protein can bind to or transport.

In the nucleotide-free inward-facing open conformation, the halves are arranged into an upside down V-shape, with the open part facing the cytosolic side of the cell. This forms a massive ~6000 $Å^3$ binding cavity that is large enough to accommodate two compounds simultaneously (Aller Stephen G. et al., 2009). The internal binding cavity contains multiple overlapping binding sites, which are likely to be coupled together through allosteric interactions. These overlapping binding sites are most likely the cause of P-gp's substrate polyspecificity (Zsila, 2007). There are 73 solvent accessible residues in this binding cavity, the majority of which are hydrophobic and aromatic residues. Only 15 residues are polar and only 2 are charged or can be potentially charged. The upper half of the drug-binding pocket consist

mainly of those hydrophobic and aromatic residues, while the lower half is dominated by more polar and charged residues (Aller Stephen G. et al., 2009). In the inward-facing open conformation, there exist two portals on the TMD's that allow entry of hydrophobic molecules into the binding cavity directly from the inner leaflet of the lipid bilayer. These portals are formed by the crossing over of TM's 4 and 5 and TM's 10 and 12. They form an intertwined structure that contributes stability to the inward-facing conformation (Aller Stephen G. et al., 2009).

At the tips of the V-shape in P-gp's inward-facing open conformation, a distance of 30 Å separates the two nucleotide binding domains (NBDs). The NBDs protrude into the intracellular side, where they are able to bind to ATP. P-gp studies with X-ray crystallography have shown that the NBDs are dimerized when bound to ATP or ATP analogs, reversing the direction of the V-shape so that the TMDs become exposed to the extracellular side (Kodan et al., 2021). This is known as the closed outward-facing conformation.

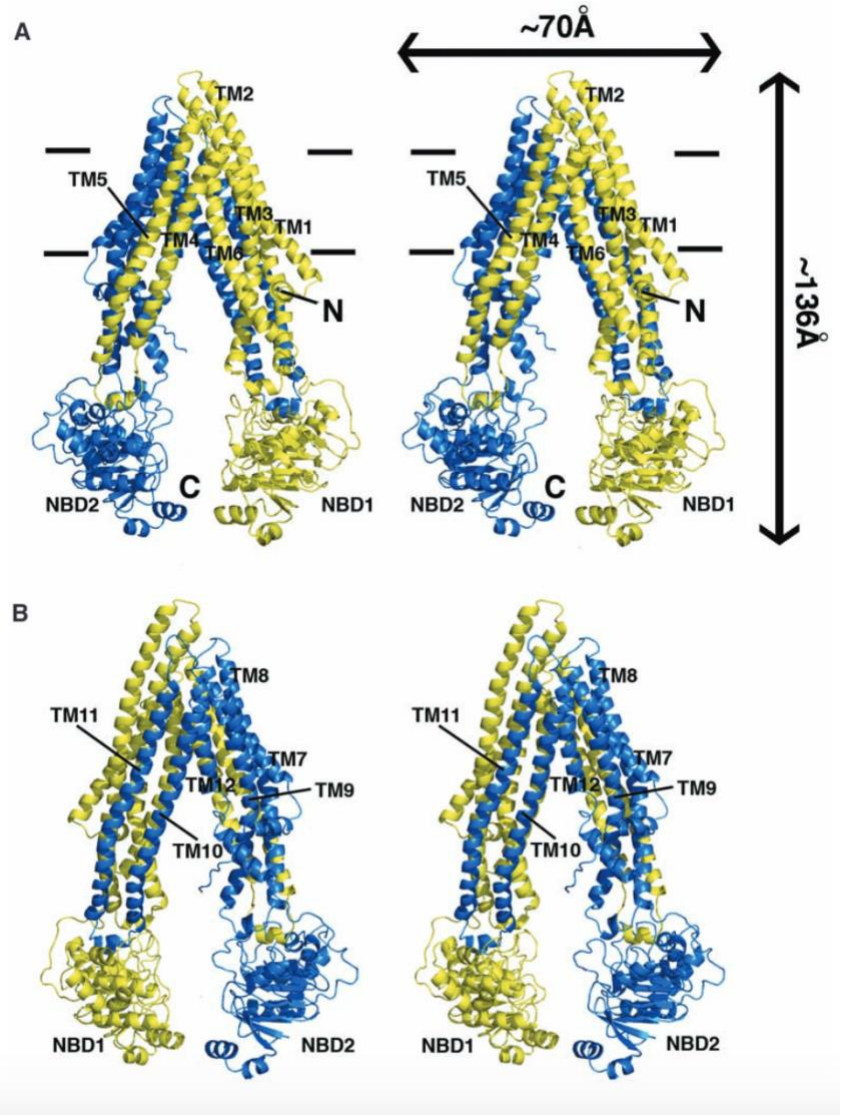

Figure 4 Structure of P-gp. (A)Frontand (B) back stereo views of PGP. TMs 1 to 12 are labeled. The N- and C-terminal half of the molecule is colored yellow and blue, respectively. TMs 4 and 5 and TMs 10 and 11 crossover to form intertwined interfaces that stabilize the inward-facing conformation. Horizontal bars represent the approximate positioning of the lipid bilayer. The N- and C-termini are labeled in (A). TM domains and NBDs are also labeled.

*Note: Figure and caption reprinted from Aller Stephen G., Yu Jodie, Ward Andrew, Weng Yue, Chittaboina Srinivas, Zhuo Rupeng, Harrell Patina M., Trinh Yenphuong T., Zhang Qinghai, Urbatsch Ina L., & Chang Geoffrey. (2009). Structure of P-Glycoprotein Reveals a Molecular Basis for Poly-Specific Drug Binding. *Science*, *323*(5922), 1718–1722. https://doi.org/10.1126/science.1168750

Mechanism of P-glycoprotein Transport

There is still much speculation around the exact mechanism of how P-gp effluxes its substrates. P-gp is known to be conformationally very fluid, a property which is vital to its effluxing action (Esser et al., 2016). Very significant movements of its NBDs have been observed throughout its catalytic cycle (Frank et al., 2016). Advances in FRET and X-ray crystallography have allowed researchers to isolate and study these conformational states. This has resulted in several models and hypotheses for how the transport mechanism occurs.

Substrate and ATP binding

The majority of P-gp's known substrates are hydrophobic and partition freely into the lipid bilayer. There is a recurring theme in P-gp literature that shows substrate extraction occurs directly from the lipid bilayer, instead of extraction from the cytoplasm (Aller Stephen G. et al., 2009) (Kim Youngjin & Chen Jue, 2018). The presence of the lateral portals exposing the binding cavity to the inner leaflet support this idea. While hydrophilic substrates can just enter the binding cavity from the cytoplasm and bind to the more hydrophilic residues in the cytosolic side of the binding cavity, hydrophobic substrates likely flow in from the inner leaflet through the portals and bind to the various binding sites consisting of the more hydrophobic and aromatic residues on the upper side of the binding cavity. The flexible helices that make up the portals are capable of closing off in the outward-facing closed conformation, likely to avoid substrate leakage back into the membrane. Either way, substrate binding reduces the structural stability of the open inward-facing conformation, putting the transporter protein in a better position to switch conformation.

Conformational change

A FRET analysis study with living cells shows that both substrate & ATP binding are required to strongly induce conformational change. Absence of either substrate or ATP returned weak FRET signals, indicating that most of the ABCB1-FRET remained in the inward-open conformational state (Kodan et al.,

2021). As ATP binding occurs at both of the NBD's, large structural changes are produced and transmitted from the NBD's to their respective TMD's, causing the conformational change that opens up the top binding cavity exposing it to the extracellular environment. Multiple sources support that conformational change from open to close and back to close is associated with twisting and bending movements at the TMD's/helices (Esser et al., 2016) (Kodan et al., 2021).

Substrate release

Depending on the compound and its binding behavior to P-gp, substrate release can be caused by several reasons: 1) hydrophilic substrates may simply diffuse out into the extracellular space; 2) hydrophobic substances may be released from the binding cavity as a result of decreased ligand:P-gp binding affinity due to conformational change. Release of substrate back into the inner leaflet is sterically blocked by the closed outward-facing conformation, which leaves little room elsewhere besides the extracellular space; 3) substrate release may be facilitated by conformational changes induced by ATP hydrolysis (Aller Stephen G. et al., 2009) (Kodan et al., 2021).

Close association of NBD's leads to ATP hydrolysis

Hydrolysis of ATP is the last step of the P-gp catalytic cycle. Close physical interaction between P-gp's nucleotide binding sites is essential for hydrolysis. Despite there being two NBD's, sources point towards a mechanism of alternating ATP hydrolysis at either NBD when they are closely associated together (Loo et al., 2012) . This is confirmed by a study that showed inhibition at one site leads to total P-gp inactivation (Esser et al., 2016). FRET analysis also confirms that ATP hydrolysis isn't involved in the conformational change from open inward-facing to closed, meaning hydrolysis doesn't lead to transport. Rather, ATP hydrolysis contributes to returning from the closed conformation to the pre-transport open conformation (Kodan et al., 2021). When ATP bonded to an NBD is hydrolyzed, the close association of the NBD's is broken off. The resulting structural changes rotates the respective TMD back to its position

in the open conformation and likely knocks off whatever bound substrate remains on the TMD's, resetting P-gp catalytic cycle back to the pre-transport state.

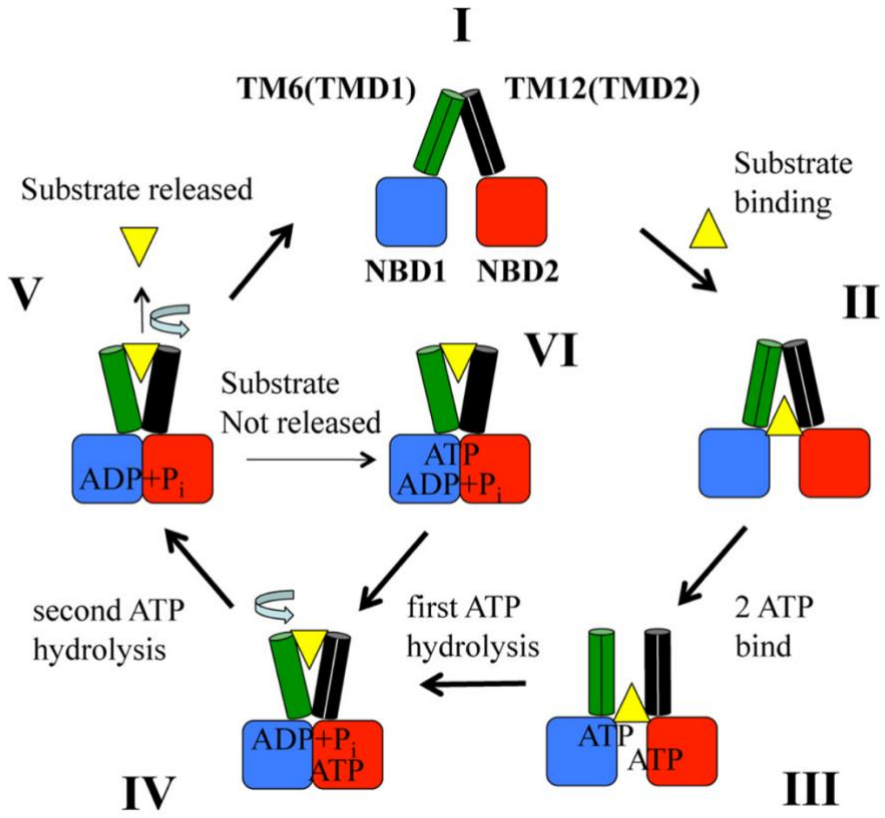

Figure 5 This figure depicts a model for P-gp's catalytic cycle. It begins with the transporter in an open inward-facing conformation (I). Binding of drug substrate and ATP can occur in random order. When the drug substrate binds, it can alter the packing of the TMD segments (II). The binding of ATP to the NBD's cause conformational changes and repacking in the TM segments, which can reduce affinity for some drug substrates (III). The binding of ATP also induces shift to outward-facing conformation (IV). After drug substrate is released, ATP hydrolysis at one of the NBD's results in the conformational shift back to inward-facing open (V). If substrate is not released, hydrolysis of the second ATP molecule causes additional changes in tertiary structure that are likely to result in drug release (VI).

*Note: Figure reprinted and caption adapted from Loo, T. W., Bartlett, M. C., Detty, M. R., & Clarke, D. M. (2012). The ATPase Activity of the P-glycoprotein Drug Pump Is Highly Activated When the N-terminal and Central Regions of the Nucleotide-binding Domains Are Linked Closely Together *. *Journal of Biological Chemistry*, *287*(32), 26806–26816. https://doi.org/10.1074/jbc.M112.376202

1.5 Pharmacokinetic Background on the 4 HIV Protease Inhibitors

Saquinavir (Invirase)

Saquinavir is a first-generation HIV protease inhibitor developed by Hoffman-LaRoche, Inc. Approved by the FDA in February 1997, it launched as a hard gelatin capsule product known as Invirase. A soft gelatin capsule product known as Fortovase was approved later that year in November (*20628ap_s007.Pdf*, 1997). *In vitro* enzymatic tests for this drug against HIV-1 protease in MT-4 cells recorded an EC_{50} of 37.7 nM for this drug. (Lv et al., 2015). Daily treatment for Invirase is 1000 mg administered twice daily with 500 mg tablets (or with 5x 200 mg capsules), in combination with ritonavir 100-mg twice daily (*020628s43-021785s19lbl.Pdf*, 2015). Some of the common side effects include nausea, vomiting, diarrhea, and fatigue. More serious side effects associated with saquinavir includes QT prolongation, heart block, high blood lipids, and liver problems. In terms of side effects, the prescribing information notes that Invirase is better tolerated than Fortovase.

Studies have been conducted to evaluate the pharmacokinetic properties of saquinavir in healthy subjects versus HIV-positive patients. For healthy volunteers the steady-state AUC, C_{max}, and C_{min} were approximately twice as high than what was observed for HIV-positive patients. The mean values for AUC and C_{max} in the control group (n=6) were 359 ± 46 ng*hr*mL^{-1} and 90.39 ± 49 ng*mL^{-1}, respectively. For the patient group, the corresponding mean values were 757.2 ± 84 ng*hr*mL^{-1} and 253.3 ± 99 ng*mL^{-1}. This difference in pharmacokinetic properties were attributed to AIDS-related hepatic impairment (*20628ap_s007.Pdf*, 1997). The bioavailability of orally administered saquinavir is about 4%.

Food has a massive effect on the pharmacokinetics for this drug. The mean 24 hour AUC after a single 600-mg oral dose was compared in fasting conditions vs. fed conditions. The 24 hr AUC measured for volunteers taking Invirase following a high-fat breakfast (1006 kcal; 48 g protein, 60 g carbohydrate,

57 g fat) was 161 ng*hr*mL^{-1}. For volunteers who took Invirase in fasted conditions, the mean 24 hr AUC was 24 ng*hr*mL^{-1}. The 24 hr AUC and C_{max} were twice as high when taken with a higher calorie meal (943 kcal, 54 g fat) vs. a lower calorie meal (355 kcal, 8 g fat). It is recommended to take Invirase within at least 2 hours after a meal. When taken without food, the plasma concentration is significantly reduced to the point that there may be no antiviral activity (*020628s43-021785s19lbl.Pdf*, 2015). In terms of distribution, saquinavir has a steady-state volume of distribution of 700 L which indicates that it partitions readily into the tissues. It is 98% bound to plasma proteins.

Renal clearance contributes a minor elimination pathway. Only 1% of saquinavir ends up getting excreted through urine. The major route of saquinavir excretion is through hepatic metabolism, mostly through the cytochrome P450 enzymes. CYP3A4 is the largest contributor to its hepatic metabolism, accounting for about 90%. Several *in* vitro studies have identified several mono- and di- hydroxylated inactive metabolites. About 88% of orally administrated saquinavir is eliminated through the feces.

Ritonavir (Norvir)

Abbott Laboratories received FDA approval for their new protease inhibitor drug in the summer of 1999. Ritonavir launched under the brand name Norvir as a soft gel capsule product. Compared to other PI drugs it is poorly tolerated. However, it has very good CYP3A suppressing ability. For this reason it is now usually taken at much smaller doses as a pharmacokinetic booster to complement other HAART drugs (Lledó-García et al., 2007). Initially, its daily treatment regimen was set at 600 mg twice daily, but current HAART regimens today will typically include only 100 mg daily of ritonavir. In terms of HIV protease inhibitory effect, its EC_{50} is about 25 nM (Lv et al., 2015). Some common side effects include diarrhea, nausea, vomiting, upper and lower stomach (abdominal pain), tingling feeling or numbness in hands and feet, rash, and fatigue (*209512lbl.Pdf*, 2017). Previous literature demonstrates that ritonavir is a P-gp substrate, but it is also a strong inhibitor as well. A cell-based assay with P-gp-expressing P388 cells determined an IC_{50} of 1.30 μM (Storch et al., 2007).

Oral bioavailability is around 65-66%; absolute bioavailability has not been determined yet in humans. Absolute bioavailability in rats was 70% (Lledó-García et al., 2007). When administered orally, bioavailability appears to be decreased under fed conditions than fasted conditions. Cmax and AUC of ritonavir decreased by 21-23% under moderately fed, high fat conditions (857 kcal, 30% from fat) compared to fasted conditions. It is 98% bound to plasma proteins and has a volume of distribution of around 20-40 L.

. Ritonavir is a potent inhibitor of CYP3A4. Therefore, extra caution must be taken when prescribing other drugs with CYP3A4 interactions. Recreational substances, fruit juices, and over-the-counter products that can modulate CYP3A4 may also put patients at risk for unexpected drug interactions. Ritonavir is also known to inhibit CYP3D6 and induces CYP1A4 (Hsu et al., 1998). 5 metabolites have been identified in human feces and urine. 3 major oxidative metabolites – M1, M2, and M11 – are formed by CYP3A. None of its metabolites are likely to contribute much to its antiretroviral effect.

Indinavir (Crixivan)

Indinavir was approved for the market in 1996. Merck & Co. branded their protease inhibitor drug as Crixivan. The *in vitro* EC_{50} with HIV-1 protease was measured to be about ~5.5 nM (Lv et al., 2015). A study to measure P-gp inhibition by HIV PI drugs determined that indinavir had very little inhibitory effect. This drug has a relatively short half-life (1.8h). Its daily treatment regimen of 800 mg needed to be spread out and taken every 8 hours. Common side effects: side effects that occurred in 2% or more of patients included “abdominal pain, fatigue or weakness, low rbc count, flank pain, painful urination, feeling unwell, nausea, upset stomach, diarrhea, vomiting, acid regurgitation, increased or decreased appetite, back pain, headache, dizziness, changes in taste, rash, itchy skin, yellowing of skin and/or eyes, upper respiratory infection, dry skin, and sore throat.” More serious side effects included kidney problems, such as kidney failure, inflammation, infection, and kidney stones. Some Crixivan

patients reported liver problems and liver failure (*020685s078lbl.Pdf*, 2016). Due to this list of severe side effects in combination with its higher pill burden, Crixivan is no longer commonly used in HAART today.

A dosing regimen of 800 mg every 8 hours found that the steady-state AUC was 30,691 ± 11,407 nM*hr (n=16), peak plasma concentration (C_{max}) was 12,617 ± 4,037 nM (n=16). At the end of the 8 hours, plasma concentration would drop off down to 251 ± 178 nM (n=16) (*020685s078lbl.Pdf*, 2016). The bioavailability of this drug was found to be approximately 65%. Food had a large effect on the absorption of this drug. It is best rapidly absorbed in the fasted state. An 84% ± 8% reduction in C_{max} and 77% ± 8% reduction in AUC (n=10) occurred when the drug was administered with a high calorie meal high and fat in protein vs. fasted. Indinavir is 60% bound to plasma protein and has a volume of distribution of 1.74 L/kg (*Indinavir PK Fact Sheet*, 2016).

In vitro studies have shown that CYP3A4 is mainly responsible for the metabolism of indinavir. Seven metabolites have been identified, none of which are considered to contribute any significant antiviral activity. In a study with 400 mg radiolabeled indinavir orally administered to healthy volunteers, about 19.1% and 9.4% of unchanged indinavir was recovered in feces and urine, respectively. In addition to being metabolized by CYP3A4, it can also act as an inhibitor albeit not as strong as ritonavir (Eagling et al., 1997).

Lopinavir (Kaletra)

Lopinavir was developed by Abbott Laboratories to build on its successful design philosophy with ritonavir (Norvir). It received FDA approval in 2000 and launched under the brand name Kaletra. Kaletra is a coformulation consisting of lopinavir and a smaller dose of ritonavir, which is used as a PK booster. Lopinavir works by the same mechanism as the other drugs by inhibiting HIV protease activity, with an EC_{50}. Its measured EC_{50} on HIV protease activity is around ~17 nM. An *in vitro* P338 cell-based assay found that LPV had some P-gp inhibitory effect, with an IC_{50} of 2.05 ± 0.2 µM (Storch et al., 2007).

The daily treatment regiment is 800 mg lopinavir + 200 mg ritonavir daily, which can be taken once daily or split up to twice daily. Common side effects include diarrhea, nausea, and vomiting. More serious ones that have been reported are pancreatitis, liver problems, hyperglycemia, immune system changes, increase in blood fat levels (such as triglycerides and cholesterol), and changes in body fat (*21-226_Kaletra_prntlbl.Pdf*, 2000).

A peak plasma concentration was measured to be 11.8 ± 3.7 μg/mL (n=24). This figure was taken from a once daily dosing regimen for four weeks with food and recorded 6 hours after administration. The AUC over a 24 hour dosing period was recorded to be 154 ± 61.4 μg * h/mL. Administration of a a 400/100 mg dose of Kaletra resulted in a mean increase of 48% and 23% in AUC and C_{max} compared to when taken in fasted conditions. It is recommended to take Kaletra tablets with food to minimize pharmacokinetic variability. Some variability and reduced exposure can occur with smaller meals. It is 98-99% bound to plasma proteins. Its volume of distribution is 61.61 L, indicating that it readily partitions into the tissue compartment (Crommentuyn et al., 2005). Absolute bioavailability has yet to be determined in humans.

Lopinavir is almost completely and exclusively metabolized by CYP3A, which necessitates its coformulation. At least 13 oxidative metabolites have been identified and studied in humans. Lopinavir can also modulate CYP3A activity as a potent inhibitor based on (Josephson, 2010).

Chapter 2

Materials and Methods

2.1 Materials

All four HIV protease inhibitor drugs in this study – Saquinavir, Ritonavir, Indinavir, and Lopinavir – were acquired through Cayman Chemicals. Special thanks to the University of Georgia's Bioexpression and Fermentation Facility, who provided the *Pichia pastoris* yeast cells that were engineered to express His-tagged wild type mouse P-glycoprotein. Ethylene glycol tetraacetic acid (EGTA) and imidazole were obtained from Alfa Aesar. Detergent *n*-dodecyl-*β*-*D*-maltoside (DDM) that is used throughout P-gp purification was purchased from EMD Millipore Corporation. Cholesterol, disodium ATP, and TRIS-HCl were all purchased from Amresco. *Escherichia coli* complete lipid extract powder was purchased from Avanti Polar Lipids Inc. Dithiothreitol (Cleland's Reagent) was purchased from Gold Biotechnology. 4-(2-hydroxyethyl)-1-piperazineethanesulfonic acid (HEPES) used in the reconstitution of liposomes was obtained from. Sodium orthovanadate was obtained from Enzo Life Sciences. Acrylamide was purchased from MilliporeSigma.

2.2 Purification of the Mouse P-glycoprotein (P-gp) Transporter

Engineered *Pichia pastoris* yeast cells were obtained from UGA's Bioexpresssion and Fermentation Facility. These yeast cells were cultivated and then induced with methanol inside a 32 1 DCI-Biolafitte fermenter with a 20:1 working capacity.

To lyse the cells, the yeast underwent a minimum of six cycles of freezing by liquid nitrogen and blending inside a commercial blender. Prior to the liquid nitrogen freezing, the liquid form of the blended yeast cells were run through a peristaltic apparatus and then dripped out as small individual dots into a vat of liquid nitrogen, which had the effect of increasing the surface area for cell lysing. The cell lysate was subjected to several rounds of centrifugation after which the pellet would be homogenized and centrifuged again at a maximum speed of 41,400 rpm.

The His-tagged wild-type mouse P-gp was isolated from the supernatant of the last ultracentrifuge cycle using a nickel-nitrolotriacetic acid (Ni-NTA) column. Previously validated protocols also include the use of diethylaminoethyl cellulose (DEAE) resin in a column to thoroughly remove impurities, but this was omitted throughout this project in order to maximize P-gp yield. Previous protein purification yields from other lab members come out to about 122 mg of P-gp per 100 grams of wet weight yeast cells, which is a comparable yield to other cited sources (Gibbs et al., 2018).

Amicon Ultra-15 100 kDa cut-off filters (EMD Millipore, Billerica, MA) were used to concentrate the protein to 150 M, after which it was kept at -80°C in a buffer consisting of 10 mM TRIS-HCl and 30% glycerol, with a pH of 8.0. The P-gp batch was screened for impurities using SDS-PAGE.

2.3 Integration of P-gp into Proteoliposomes

Pure P-gp will not function reproducibly unless in the presence of lipids. The P-glycoprotein was reconstituted into 400 nm unilamellar liposomes in order to facilitate studying the protein in the context of cell. This was accomplished using a method of extrusion through a 400 nm filter. The liposome mixture consisted of 80% w/v Avanti *E. coli* Total Lipid Extract (Avanti Polar Lipids) and 20% w/v cholesterol. Avanti Total *E. coli* Lipid Extract was used because it demonstrated good ATP hydrolysis activity in previous investigations of mouse P-gp (Loo & Clarke, 2016) (Lerner-Marmarosh et al., 1999). Other studies also showed that 20% w/v cholesterol improved P-gp ATPase activity, so this ratio was ultimately chosen for the liposome mixture (Eckford & Sharom, 2008) (Rothnie et al., 2001).

The liposome solution was made in advance to P-gp reconstitution. This was done by dissolving the combined lipids and cholesterol in 10 mL of chloroform, leading to a concentration of 10 mg mL^{-1}. This chloroform solution was allowed to evaporate over the course of 1 hour using a Buchi Rotovapor Model R-114 (Buchi) In doing so, the remaining lipids and cholesterol mixture formed a thin film on the bottom of the flask which was resuspended in 10 mL of a rehydration buffer (50 mM Tris/HCl, 0.1 mM EGTA, pH 7.4). To get the organic film to fully dissolve in the rehydration buffer, liquid nitrogen was used to freeze and thaw the suspension for at least 10 cycles. This rehydrated liposome solution was then taken through the extrusion process to achieve a more consistent liposome size. This extrusion was performed using a Millipore 400 nm cutoff filter (EMD Millipore) on a LIPEX extruder (Northern Lipids) for a total of 11 cycles. Prior to the reintegration, the DDM-solubilized P-gp (~100 uM) was dialyzed against HEPES buffer (20 mM HEPES, 100 mM NaCl, 5 mM $MgCl_2$, 2 mM DTT, pH 7.4) for 2 hours to remove excess detergent. After that, the P-gp and extruded liposomes were finally combined to a final concentration of ~50 µM and 4 mg mL^{-1}, respectively. This mixture was allowed to incubate on ice for 1 hour. Following this incubation, a second round of dialysis against HEPES buffer for 2 hours was done to facilitate the integration of P-gp into the liposomes. This prepared proteoliposome solution was then aliquoted and stored at -80°C. The colorimetric DC Protein Assay was used to determine protein concentration for each batch of proteoliposomes (Bio-Rad).

2.4 Assay for P-gp ATPase Activity

The colorimetric ATPase activity assay was used to assess the Pgp-mediated ATP hydrolysis in the presence of the four HIV protease drug substrates (Chifflet et al., 1988). This assay measures enzymatic activity by utilizing a molybdenum solution which reacts with free inorganic phosphate (P_i) that is released as a result of ATP-dependent substrate transport. The formation of the P_i-molybdenum complex results in a change in color that causes a strong and measurable absorbance signal at 850 nm.

All data for these experiments were measured and recorded on a BMG LabTech CLARIOStar Microplate Reader. The ATPase activities of the four HIV protease drugs saquinavir, ritonavir, indinavir, and lopinavir were assessed on a 96-well microplate in the presence of 50 nM P-gp reconstituted into proteoliposomes. A range of drug concentrations ranging from 500 to 0 µM was tested, with a standard curve established using known concentrations of potassium phosphate. The known P-gp inhibitor sodium orthovanadate was used as negative control (Urbatsch et al., 1995). Chifflet buffer (150 mM NH_4Cl, 5 mM $MgSO_4$, 0.02% wt/vol NaN_3 and 50 mM TRIS/HCl, pH 7.4) was used to dilute all reagents on the microplate to the correct concentrations.

Nonlinear regression was used to fit the ATPase kinetics data of the four drugs using Igor Pro 9 (Wavemetrics, Tigard, OK). A modified Michaelis-Menten equation is used to fit monophasic P-gp ATPase kinetics, in which V represents rate of ATP hydrolysis, V_{sat} is the maximum rate of ATP hydrolysis at saturating drug concentration, [L] is the ligand or drug concentration, K_m is the Michaelis-Menten constant, and V_{basal} is the basal ATP hydrolysis rate.

$$v = \frac{V_{max}[L]}{K_m + [L]} + v_{basal}$$

Equation 1

For biphasic curves, the following substrate inhibition equation was used, where K_I is the inhibitory constant.

$$v = \frac{V_{max}[L]}{1 + \frac{K_m}{[L]} + \frac{[L]}{K_I}} + v_{basal}$$

Equation 2

For a biphasic kinetics curves exhibiting a sigmoidal shape instead of inhibition, the Hill equation is used.

$$v = \text{base} + (\max - base)/\{1 + \left[\frac{xhalf}{x}\right]^{rate}\}$$

Equation 3

For triphasic kinetics curves, a combination of the Hill and Michaelis-Menten equation was used to fit the data, where N is equal to the number of binding spots.

$$v = \frac{(V_1 * L^N)}{(K_1^N + L^N)} + \frac{(V_2 * L)}{(K_2 + L)} + V_{basal}$$

Equation 4

In practice, only the equations for biphasic and triphasic curves was used for curve fitting in this project, as the kinetics for the HIV protease drugs only exhibited biphasic and triphasic behavior.

2.5 Measuring P-gp:Drug Affinity using Tryptophan Fluorescence Quenching

Quenching of intrinsic protein fluorescence emitted by tryptophan residues was used as a method to determine the dissociation constants of the various P-gp:drug complexes. As a result, this method gives a closer look into the binding affinity of P-gp with each of the HIV protease drugs in this study. An Olis DM 45 spectrofluorimeter (Olis Corporation, Bogart, GA) was used for these P-gp tryptophan quenching experiments. As drug was slowly titrated in over a determined range, the fluorescence emission of P-gp was measured from 300-500 nm, with excitation at 295 nm followed by emission at 330 nm. This drug titration was performed in Chifflet buffer within a 1 cm path length quartz cuvette. Background, volume, and inner filter effects were taken into consideration when calculating the actual degree of P-gp fluorescence quenching caused by drug binding. In the following equation, F

represents the observed fluorescence count of the protein at 333 nm after excitation at 295 nm, B is the background of the Chifflet buffer in the cuvette, [Q] is the ligand concentration, and ε_{ex}, ε_{em}, b_{ex}, and b_{em} represent the excitation and emission extinction coefficients and the excitation and emission pathlengths.

$$F_{corrected} = (F - B)10^{\frac{(\varepsilon_{ex})(b_{ex})+(\varepsilon_{em})(b_{em})[Q]}{2}}$$

Equation 5

Extinction coefficients for all four drugs were determined experimentally; the drugs were essentially transparent within the working concentrations, so the contribution of extinction coefficients was minimal. Ritonavir and lopinavir showed evidence of increasing fluorescence emission within the range of their working concentrations, so that background was also subtracted to determine the true degree of drug-induced tryptophan quenching. This increase in fluorescence emission in samples of just drug and solvent were not observed in saquinavir nor indinavir.

Quenching of tryptophan fluorescence can occur by 2 major mechanisms: static and dynamic quenching. Static quenching describes drug-induced quenching that is caused by binding between the drug ligand and P-gp. This provides a direct picture of the drug's affinity for the protein. Dynamic quenching describes quenching that is caused by random collisions between -Pgp and ligand. In order to simulate the environments that could induce the two different mechanisms, quenching experiments were performed in 21°C and 37°C. The differences between the quenching patterns was observed to ascertain whether the drug underwent both mechanisms or just static quenching.

Regardless of the mechanism for quenching, the curves for tryptophan quenching data were fitted to equation 5, in which $F_{corrected}$ represents the corrected fluorescence, $F_{corrected,0}$ represents fluorescence of the 1 uM P-gp with no drug present, K_{SV} is the Stern-Volmer constant, and [Q] is concentration of the quenching ligand.

$$F_{corrected} = \frac{F_{corrected,0}}{1 + K_{SV}[Q]} + F_{unquenched}$$

Equation 6

In the dynamic quenching mechanism, an increase in temperature would be accompanied by an increase in K_{SV}. This is a result of the increase in random particle collision between quenching drug and P-gp. In contrast, the static quenching model would exhibit an inverse relationship between temperature in K_{SV} (Lakowicz, 2006).

2.6 Determining Tryptophan Residue Accessibility using Acrylamide as Quencher

Acrylamide quenching builds upon the existing method of tryptophan fluorescence quenching through a slight modification. Acrylamide is a polar molecule that is not capable of penetrating lipid bilayers nor the hydrophobic interior of proteins. In this case, acrylamide acts as the quencher of P-gp tryptophan fluorescence, instead of the HIV drug. For these experiments, acrylamide is slowly titrated in over a certain range while the concentration of the substrate being studied is held constant, and the fluorescence of the P-gp is measured at 333 nm after excitation at 295 nm. This technique is used to explore the accessibility of tryptophan residues within P-gp; this accessibility is dependent upon conformational changes in P-gp's tertiary structure, that can be induced by drug binding. The greater the solvent accessibility, the wider the conformational state.

To ascertain the degree of non-specific quenching, experiments with N-acetyl-L-tryptophanamide (NATA) were performed as a control instead of using P-gp. This is because NATA' structure is composed of tryptophans that are freely accessible to aqueous solvent. Acrylamide quenching of P-gp in absence of drug substrate (apo-Pgp) provided a control for the open conformation state. A non-hydrolyzable analogue of ATP, adenylyl-imidodiphosphate (AMP-PNP), was used as the

control for P-gp's closed conformation. This analogue binds to the NBD's. Because it cannot be hydrolyzed, AMP-PNP prevents the protein from reverting into its open pre-transport state.

Just as with regular tryptophan quenching data, Equation 4 was used to adjust fluorescence intensities for inner filter effects and background. Stern-Volmer plots were created by plotting $F_{corrected,0}/F_{corrected}$ against acrylamide concentration, with $F_{corrected,0}$ representing the fluorescence of P-gp in absence of acrylamide quencher. In the rearranged Equation 5, the relationship between the slope of the Stern-Volmer plots and K_{SV} is shown more clearly, with K_{SV} being equal to the slope. The value for K_{SV} is taken as an estimation of the degree of tryptophan quenching by an acrylamide titration.

$$\frac{F_{corrected,0}}{F_{corrected}} = 1 + K_{SV}[Q]$$

Equation 7

Chater 3

Results

3.1 The kinetics of Pgp-coupled ATPase Hydrolysis Induced by HIV Protease Inhibitors

Consumption of ATP is a widely-used measure of ABC transporter activity. In the process of pumping out exogenous substrates out of cells, typically against a concentration gradient, the membrane transporter will hydrolyze ATP into ADP. The subsequent increase in inorganic phosphate concentration is detectable through the Chifflet method (Chifflet et al., 1988). P-gp is no exception to this characteristic of its transporter family. That increase in inorganic phosphate is coupled to P-gp activity. To get a clear picture of P-gp's ATPase activity with each drug, a range of doses for each drug was plated with 50 nM P-gp, in the presence of ATP at a saturating concentration of 3.2 mM. Previous studies on P-gp with various concentrations of ATP found that the enzyme reached maximal activity around this concentration. Studying P-gp's ATPase activity with each drug allows for extracting useful kinetics parameters that would allow for the comparison of each substrate's transport rate and affinity for P-gp

Equation 1 was used to fit the curves to estimates of the kinetic parameters. Figure 6 displays the kinetics curves for all four drugs, along with important kinetics parameters. Table 2 lists all the kinetic parameters that were extracted from the fitting of each curve. Because they required different equations, these parameters

Saquinavir-induced P-gp ATP hydrolysis resulted in a K_m of 2.11 ± 0.71 µM and a V_{max} of 768.51 + 1.36e+03 nmol min^{-1} mg^{-1}. For Ritonavir P-gp ATP hydrolysis, the K_m was 9.04 ± 3.66 µM and the V_{max} reached 1298.84 nmol min^{-1} mg^{-1}. Indinavir P-gp ATPase kinetics had a K_m of 3.61 ± 1.17 µM and the V_{max} reached 722.25 ± 57.9 nmol min^{-1} mg^{-1}. For Lopinavir, its P-gp ATPase kinetics had a K_m of 2.43 ± 0.39 µM and the V_{max} reached 815.77 ± 717 nmol min^{-1} mg^{-1}.

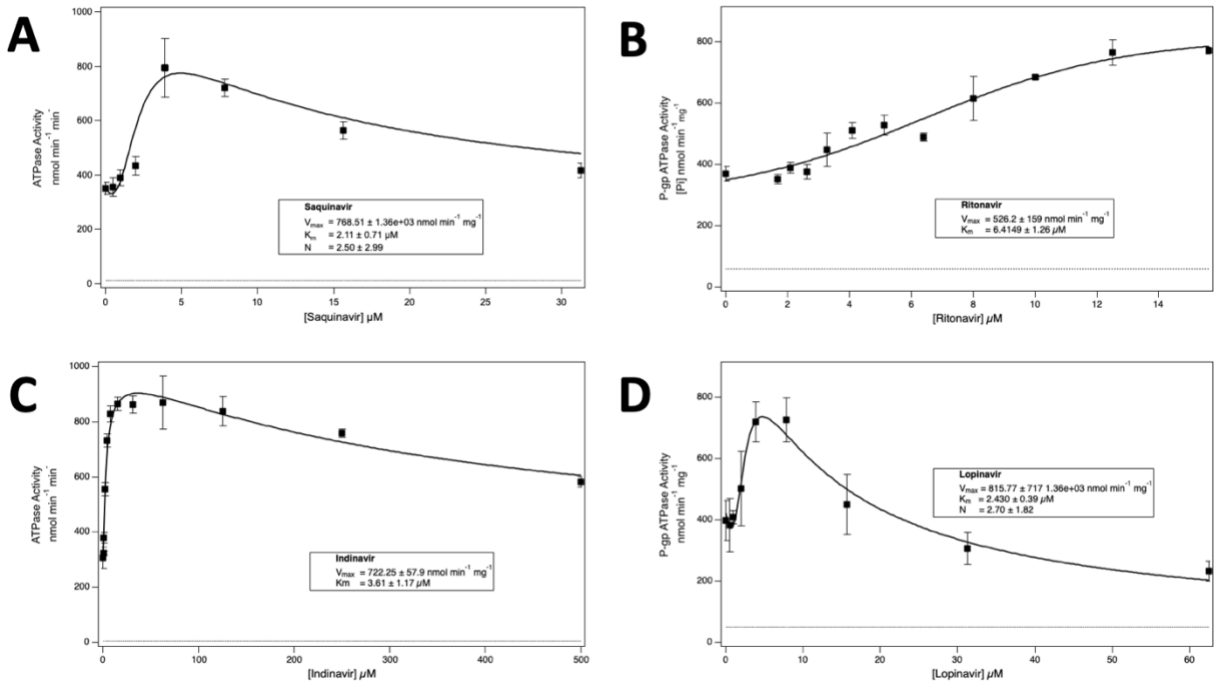

Figure 6 The ATPase activity of 50 nM P-gp in the presence of 3.2 mM sodium ATP and a range of concentrations of the HIV inhibitors A) saquinavir, B) ritonavir, C) indinavir, D) lopinavir. Data for $NaOVO_3$ in the same conditions represents negative control as dashed line. The vertical error bars indicate the standard deviation across triplicate experiments, while the dotted data points represent the average of at least 3 trials.

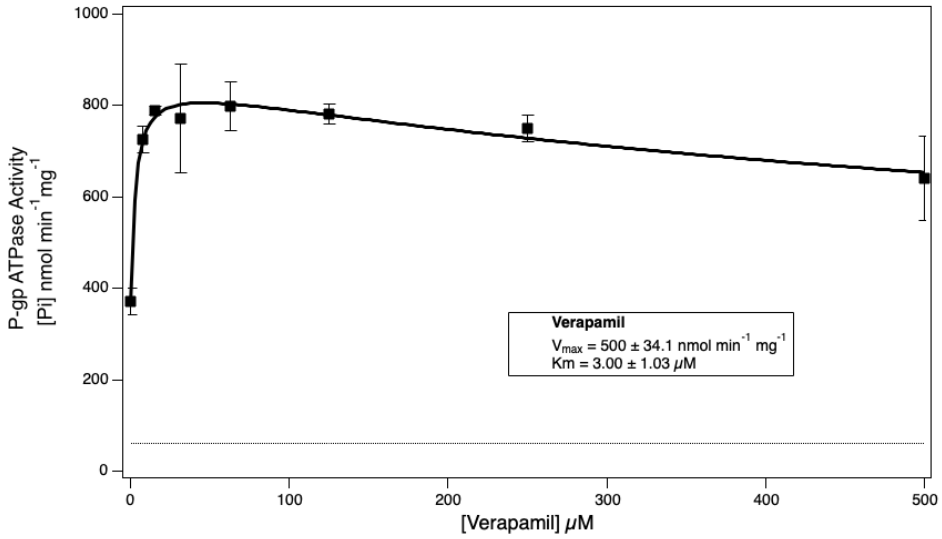

Figure 7 The ATPase activity of 50 nM P-gp in the presence of 3.2 mM sodium ATP and a range of concentrations of verapamil. Data for $NaOVO_3$ in the same conditions represents negative control as dashed line. The vertical error bars indicate the standard deviation across triplicate experiments, while the dotted data points represent the average of at least 3 trials

Figure 7 shows P-gp ATPase kinetics of verapamil. This drug is known for being both an inhibitor and a transported substrate of P-gp. Verapamil has been used as a control for this experiment due to its well-documented biphasic ATPase kinetics, which exhibits an activation and an inhibition stage (Ledwitch & Roberts, 2017). This kinetics curve has a K_m 3.00 ± 1.03 µM and V_{max} of 500 ± 34.1 nmol min^{-1} mg^{-1}. Both ritonavir and indinavir also exhibited two-phase ATPase kinetics, with indinavir being especially close to verapamil's. Saquinavir and lopinavir exhibited three-phase kinetics, which required a combined Hill and Michaelis-Menten equation to properly fit. Out of all the HIV protease inhibitors in this study, saquinavir had the smallest K_m value, indicating that it has the fastest transport rate. In order from smallest K_m value to biggest, the the drugs ordered as saquinavir > lopinavir > indinavir > ritonavir.

Table 1 Kinetic Parameters of each drug

	Saquinavir	**Ritonavir**	**Indinavir**	**Lopinavir**
K_m (μM)	2.11 ± 0.71	9.04 ± 3.66	3.61 ± 1.17	2.43 ± 0.39
V_{max} (nmol min^{-1} mg^{-1})	768.51 + 1.36e+03	1298.84	722.25 ± 57.9	815.77 ± 717

Table 2 Raw kinetic parameters extracted directly from equation fitting. Parameters are different because RTV was fitted using the Hill equation (Equation 3), while SQV and LPV were fitted using modified Hill/Michaelis-Menten equation (Equation 4).

Saqinavir	**V_{basal}**	**V_1**	**V_2**	**K_1**	**K_2**	**N**
	348.± 57.1	768.51 ± 1.36e+03	-874.68 ± 1.02e+03	2.11 ± 0.71	44.1 ± 11.62	2.99 ± 2.5
Lopinavir	**V_{basal}**	**V_1**	**V_2**	**K_1**	**K_2**	**N**
	421.87 ± 47.6	815.77 ± 717	-1200 ± 678	2.43 ± 0.39	10 ± 11.3	2.70 ± 1.82
Ritonavir	**base**	**max**	**x-half**	**rate**		
	354.11 ± 31.8	944.73 ± 210	9.03 ± 3.66	1.88 ± 0.74		

3.2 Determining the binding affinity of P-gp and Substrate Using Intrinsic Tryptophan Quenching

Saquinavir was the only drug to exhibit significant tryptophan quenching with a K_d of 6.20 ± 0.1 µM, which is displayed in Figure 8. The other three drugs did not quench intrinsic tryptophan, so estimation of K_d for these drugs was not possible. Due to saquinavir and lopinavir exhibiting three-phase inhibitory P-gp at saturating concentration, a competition experiment was performed to determine whether the drugs shared the same third binding spot. This experiment was performed with 10 µM saquinavir as a probe vs. lopinavir slowly titrated in as a competition quencher up to 16 µM. No competition quenching was observed in this experiment, implying that the two drugs may have different inhibitory binding sites.

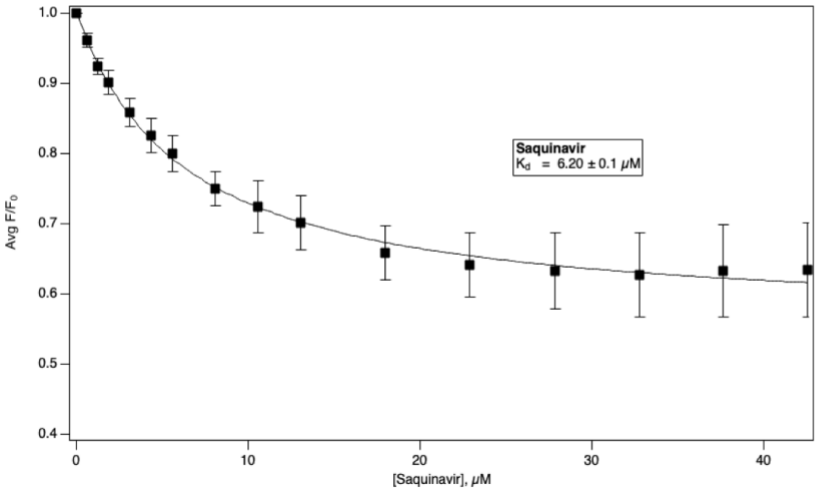

[SQV]	Average Relative Fluorescence Units	STD DEV
0	97595	663.51
0.62	93101	1562.03
1.25	88757	1481.36
1.87	85781	1924.8
3.12	80181	1729.04
4.36	75764	2232.6
5.6	72128	2246.44
8.08	65413	1934.93
10.55	60926	2801.88
13.02	56924	2716.26
17.96	49945	2503.26
22.9	45387	2687.8
27.82	41696	2911.68
32.73	38583	3030.68
37.64	36222	3018.71
42.53	33930	2888.41

Figure 8 The degree fluorescence emission quenching of P-gp @ 330 nm by increasing concentration of saquianvir , expressed as fluorescence emission (F) divided by the starting fluorescence (F_0). Equation 4 was used to correct for background and the inner filter effect to get F at each titration point. Each data point indicates the average of three experiements while error bars show the standard deviation across three experiments. Equation 5 was used to fit the data and to estimate the K_d. The raw data is shown on the right.

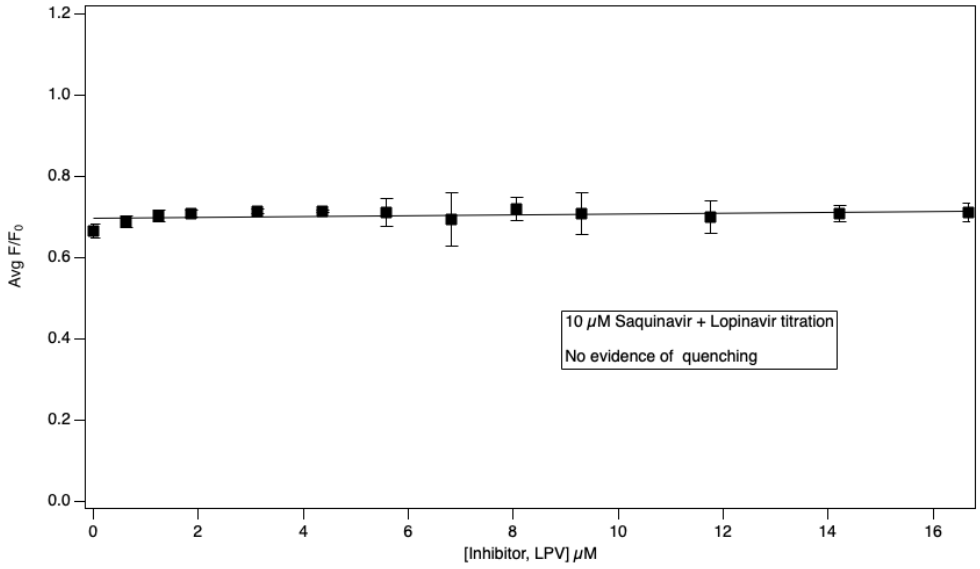

Figure 9 Competition experiment with 10 μM saquinavir as probe and lopinavir titrated in as competition. Starting fluorescence (F_0) at 0 μM LPV is omitted to avoid confusion. Each data point indicates the average of three experiements while error bars show the standard deviation across three experiments. Fitted with equation of straight line to show no quenching ocurred.

3.3 Evaluating P-gp Conformational Changes in Presence of HIV Protease Inhibitors Using Acrylamide as Quencher

In this experiment, acrylamide titrations at a set concentration of each drug was used to investigate the drug-induced conformational changes that affect solvent accessibility. The greater the solvent accessibility, the wider the P-gp conformational state. The slopes of the Stern-Volmer plots (K_{sv} values) go hand in hand with solvent accessibility. To summarize, the higher the Ksv value, the greater the solvent accessibility, the greater the quenching of tryptophan fluorescence, and the wider the conformational state adopted by P-gp.

Figure 10 displays the three controls used for this experiment: the NATA control, the Apo-Pgp control, and the AMP-PNP control. The NATA control represents a fully quenchable analogue with complete solvent accessibility that reflects P-gp's 11 tryptophans, which had a K_{sv} of 18.246 ± M^{-1}. The apo-Pgp control, which represents P-gp in the open conformation in absence of drug, yielded a K_{sv} of

1.51 ± 0.14 M^{-1}. The AMP-PNP control, which locks P-gp in the closed conformation, yielded a K_{sv} of 1.17 ± 0.09 M^{-1}.

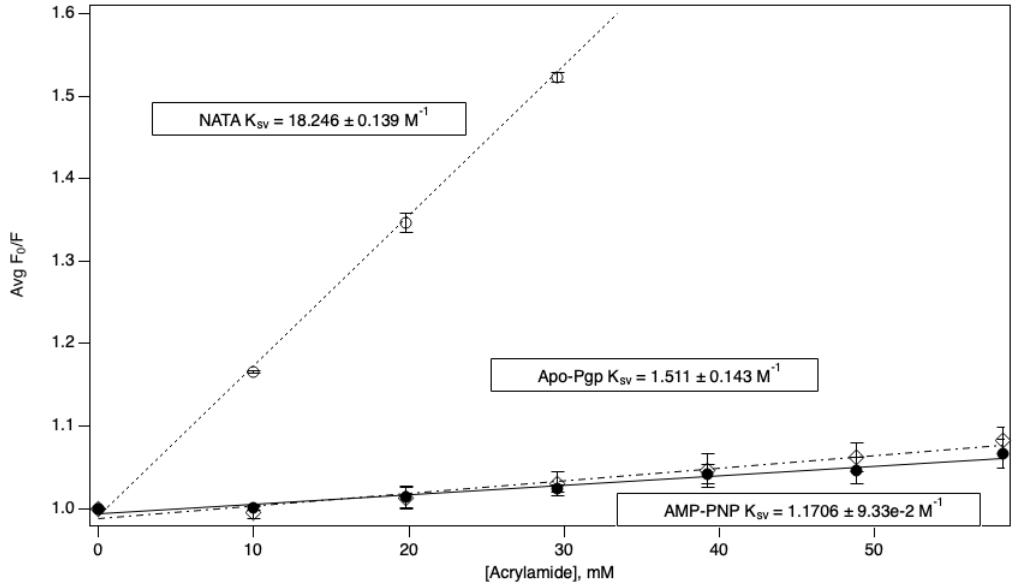

Figure 10 The Stern-Volmer plots and respective K_{sv} values for the three controls NATA (open circle, dotted line), apo-Pgp (open diamond, dashed line), and AMP-PNP (closed circle, normal line). Each data point indicates the average of three experiements while error bars show the standard deviation across three control experiments.

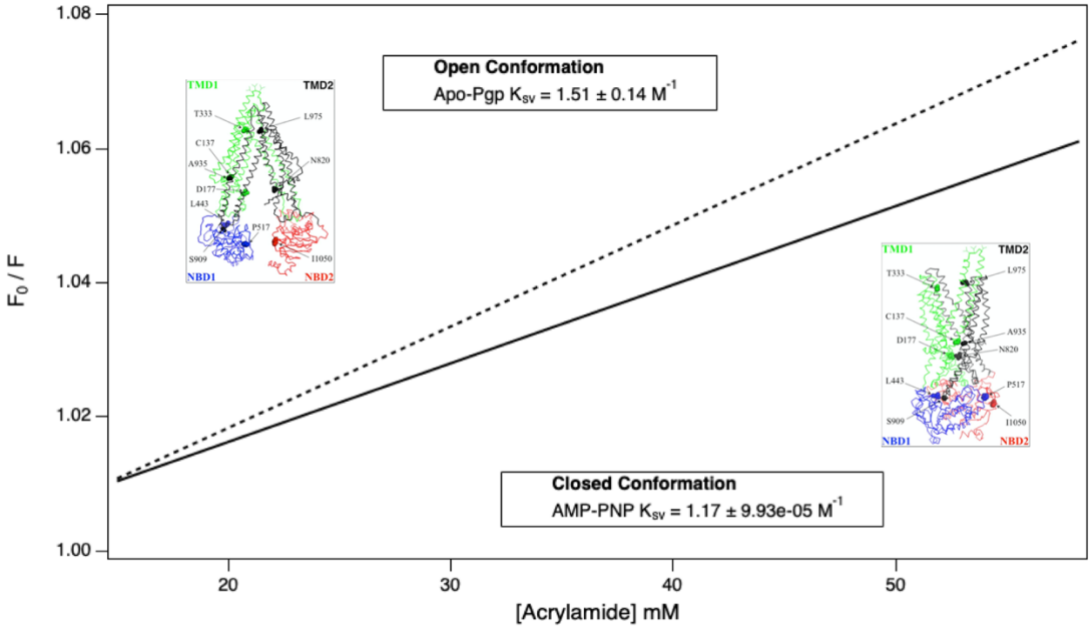

Figure 11 Stern-Volmer plots for just Apo-Pgp and AMP-PNP, their respective K_{sv} values, and conformational states. This better visualizes the separation between the two controls, as NATA quenching is far beyond what is expected to be observed.

Figure 12 shows the Stern-Volmer plots for P-gp in various concentrations of lopinavir. For the sake of readability, the K_{sv} values that were recorded from the rest of the acrylamide quenching experiments for the other drugs are all represented on bar graphs.

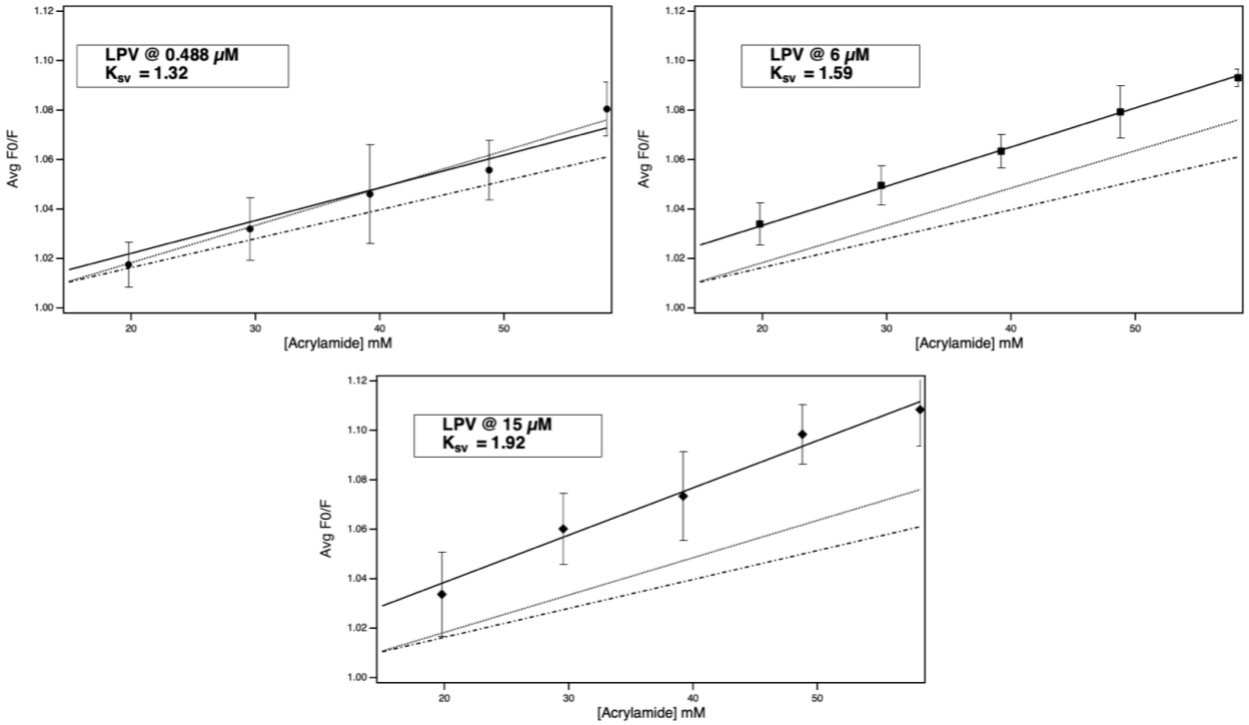

Figure 12 This represents three Stern-Volmer plots for acrylamide quenching experiments of P-gp at 0.488 μM (open square),, 8 μM (open circle), and 16 μM lopinavir (closed circle). Each data point represents the average of 3 different experiments at each drug concentration. Error bars show the standard deviation across three experiments.

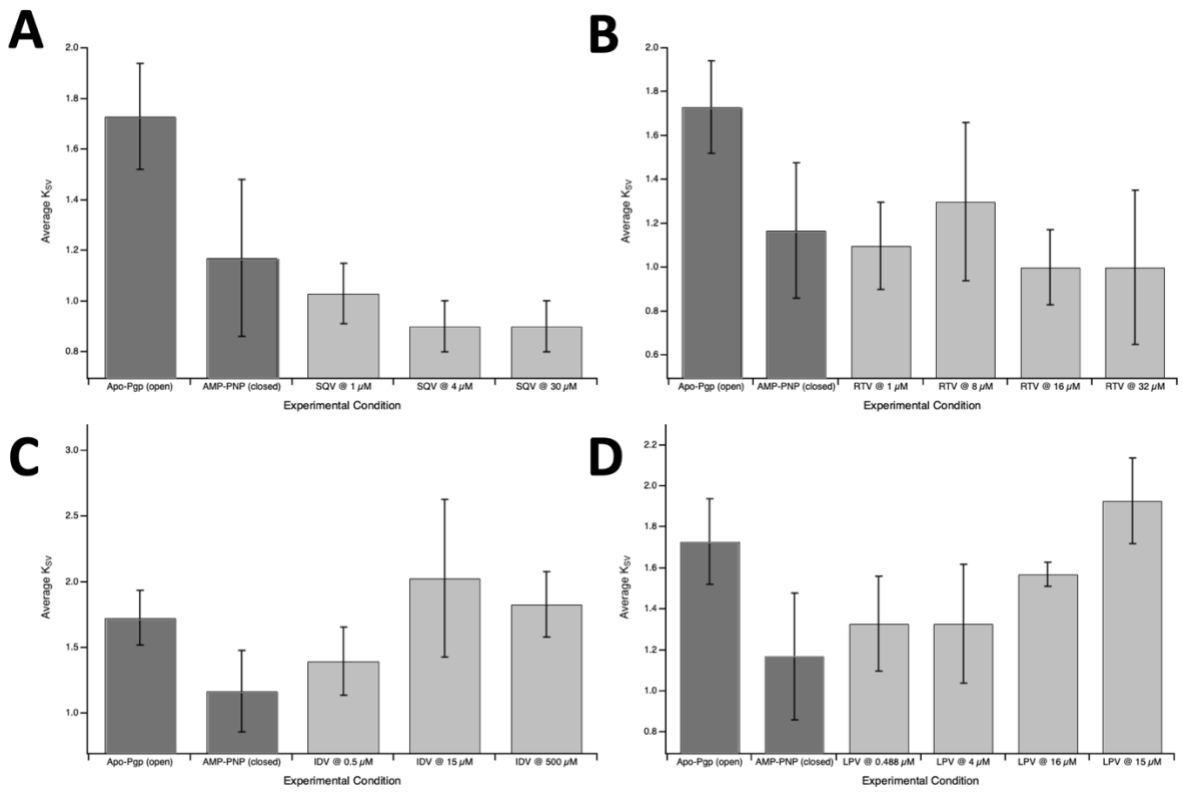

Figure 13 Acrylamide quenching of P-gp in various concentrations of A) saquinavir, B) ritonavir, C) indinavir, and D) lopinavir. The bar graphs represent the average of K_{sv} values from three experiments at each drug concentration. The controls for open and closed conformation are included as the first two dark gray bars. Error bars indicate the standard deviation of those three $K_{SV.}$ values.

Figures 13 A-D summarizes the K_{sv} values for acrylamide quenching of P-gp in various concentrations of saquinavir, ritonavir, indinavir, and lopinavir, respectively. In increasing concentrations of saquinavir, solvent accessibility decreased. The K_{sv} values did not change much, staying below the AMP-PNP control of 1.17 ± 0.31 M^{-1}. This implies that P-gp shifts towards a more closed conformation that restricts acrylamide accessibility (Figure 12-A). In acrylamide quenching experiments with ritonavir, solvent accessibility decreased slightly with increasing concentrations of drug. The K_{sv} values shifted slightly below the AMP-PNP control, reaching a minimum of 1.0 ± 0.17 M^{-1} (Figure 12-B). For indinavir, solvent accessibility increased significantly with higher concentrations of drug – even beyond the apo-Pgp control of 1.73 0.21 M^{-1} for open conformation. The highest K_{sv} value recorded was 2.03 ± 0.6 M^{-1} (Figure 12-C). For lopinavir, solvent accessibility steadily increased with

higher concentrations of drug, similar to indinavir. However, it doesn't reach quite as high a K_{sv}, reaching a max of 1.93 ± 0.21 M^{-1} at its highest concentration (Figure 12-D). The changes in K_{sv} show that P-gp adopts conformational changes induced by the presence of various concentrations of drug.

Chapter 4

Discussion

Altogether, the data from the ATPase hydrolysis experiments and the quenching experiments paint an interesting picture of how HIV PI's interact with P-gp. There were several surprising results. Triphasic ATPase activity curves were observed with saquinavir and lopinavir. This indicates that the two drugs have at least 3 binding sites with P-gp. What was more surprising about this data was that inhibition of enzyme activity was seen at the third phase at higher saturating concentrations for both drugs. To determine if whether saquinavir and lopinavir shared the same third binding spot, a competition tryptophan quenching experiment was performed with saquinavir as a probe and with lopinavir titrated in as an inhibitor. This experiment ruled out the possibility of both drugs having the same inhibitory third binding spot. For the remaining 2 drugs, ritonavir and indinavir displayed biphasic ATPase activity kinetics, which indicated two binding sites. No significant dip in P-gp ATpase activity was observed after the initial lag phase which rules out inhibition, at least within the soluble ranges for either drug.

From this data, a triple vs. dual occupancy model for HIV PI drugs arises. Triple occupancy of HIV PI's on P-gp leads to inhibition of activity at saturating concentrations of drug. Double occupancy leads to positive cooperativity and maximal enzyme activation**.** This model is based on what we know about the P-gp catalytic cycle in the presence of ATP, and the previously described behaviors of the nucleotide binding domains (Kim Youngjin & Chen Jue, 2018) (Loo et al., 2012). The triple occupancy drugs –

saquinavir and lopinavir – likely bind to lower-affinity allosteric sites. Two pieces of evidence point to different inhibitory third binding sites: 1) drastically reduced ATPase activity was observed in the third phase of the kinetics data for both drugs at saturation, however increased P-gp solvent accessibility was observed in higher concentrations of lopinavir, whereas decreased P-gp solvent accessibility was observed in higher concentrations of saquinavir and 2) their lack of competition tryptophan quenching. The competition tryptophan quenching experiment does not exhaustively prove a lack of competition between the two, but merely implies it. Previous studies working with HIV PI drugs postulated the idea of three binding sites and potential allosterically-coupled inhibitory binding sites (Bierman et al., 2010) (Zsila, 2007). They also support the idea that these drugs do not inhibit competitively at all, whether *in vitro* or *in vivo* (van der Sandt et al., 2001).

The reduced P-gp solvent accessibility observed in higher concentrations of saquinavir indicate a closed off conformation, which is confirmed by the low K_{SV} values that were observed. Because ATPase activity still maintains slightly above basal activity, even in the inhibition phase - there must be some interaction of the NBDs for hydrolysis to occur. Higher concentrations of saquinavir lock P-gp into an intermediate conformation instead of closed conformation, despite the low Ksv. For lopinavir, the solvent accessibility appears to shift higher with increasing drug concentration. Combined with the very low sub-basal ATPase activity at saturation, it can be concluded that P-gp is locked into a very wide open inward-facing conformation in which the nucleotide tide binding domains are completely separated. With the NBDs unable to interact, P-gp's catalytic efflux cycle is frozen due to the hydrolysis of ATP coming to a stop, despite the saturating presence of substrate.

A previous study with verapamil and ATP cooperativity proposed a double occupancy positive cooperativity model for P-gp. It was demonstrated that verapamil binded to two separate sites on P-gp, which stabilizes an intermediate conformation in which the NBD's are closer together than in the open conformation, but not as close as in the closed conformation (Ledwitch et al., 2016). Specifically, the low

affinity site that is closer to the center of the protein might be causing stearic hindrance, preventing the NBD's from coming together completely. However, increased stability of this middle ground conformation also prevents P-gp from pushing all the way to closed conformation, which can only be reached when the distance between the NBD's is minimal. This is likely what is happening in the case of lopinavir, except that it is the very wide open conformation that is allosterically stabilized by the binding of the drug to the third binding site, as opposed to stabilization of the intermediate conformation.

The behavior of the double occupancy drugs – ritonavir and indinavir – also showed differences in shifts in solvent accessibility. For ritonavir, the K_{sv} values leaned towards the AMP-PNP control, and there wasn't much variability. In combination with the ATPase data, this indicates that the P-gp conformational states were similar. It is likely that P-gp adopts an intermediate conformation at lower concentration and then a closed conformation with the NBD's in close proximity at higher concentration. The binding of the drug at the second binding site induces maximal activity. For indinavir, the K_{sv} values shifted beyond the apo-Pgp control for open conformation at the higher concentrations. Taken within the context of its ATPase kinetics, this free solvent accessibility is likely due to a wide open *outward*-facing conformation. While the NBD's are in close association, the outward facing conformation is so wide open that the internal hydrophobic cavity becomes accessible to solvent from the outside. Indinavir-induced P-gp ATPase kinetics reaches peak activity in its second phase right at around 50 µM, followed by a very slow inhibitory decline observable up to its maximum solubility point of 500 µM. This is reflected in the slight decrease in solvent accessibility from the acrylamide quenching experiments at 15 µM to 500 µM, which implies that the NBD's revert towards a slightly more intermediate conformation. This theme of positive cooperativity with double occupancy can be seen in other ABC transporters. *In vitro* studies with paclitaxel and BCRP indicate that binding of the drug in two distinct sites is required to reach maximal levels of active transport (BROOKS et al., 2004).

One interesting thing to note is that multiple cell-based studies quote ritonavir as a strong potential inhibitors for P-gp activity out of the HIV PI drugs (Bierman et al., 2010) (Storch et al., 2007) (Zolnerciks et al., 2011). However, ritonavir-induced inhibitory effect on the ATPase kinetics was not observed, at least within the soluble range of the drug. The kinetics data took on a sigmoidal shape, being the only drug that did so. This could be attributed to the fact that the ATPase activity assay doesn't directly measure efflux or transport – it measures ATP hydrolysis, which is usually tied to transport. Ritonavir may exert its inhibitory effect on P-gp efflux through an allosteric interaction that promotes the closed conformation and therefore ATP hydrolysis, not necessarily being transported efficiently itself (Loo et al., 2012). A different study involving a transport assay alongside the ATPase assay will be required to distinguish the contribution of true efflux to ritonavir's P-gp ATPase kinetics.

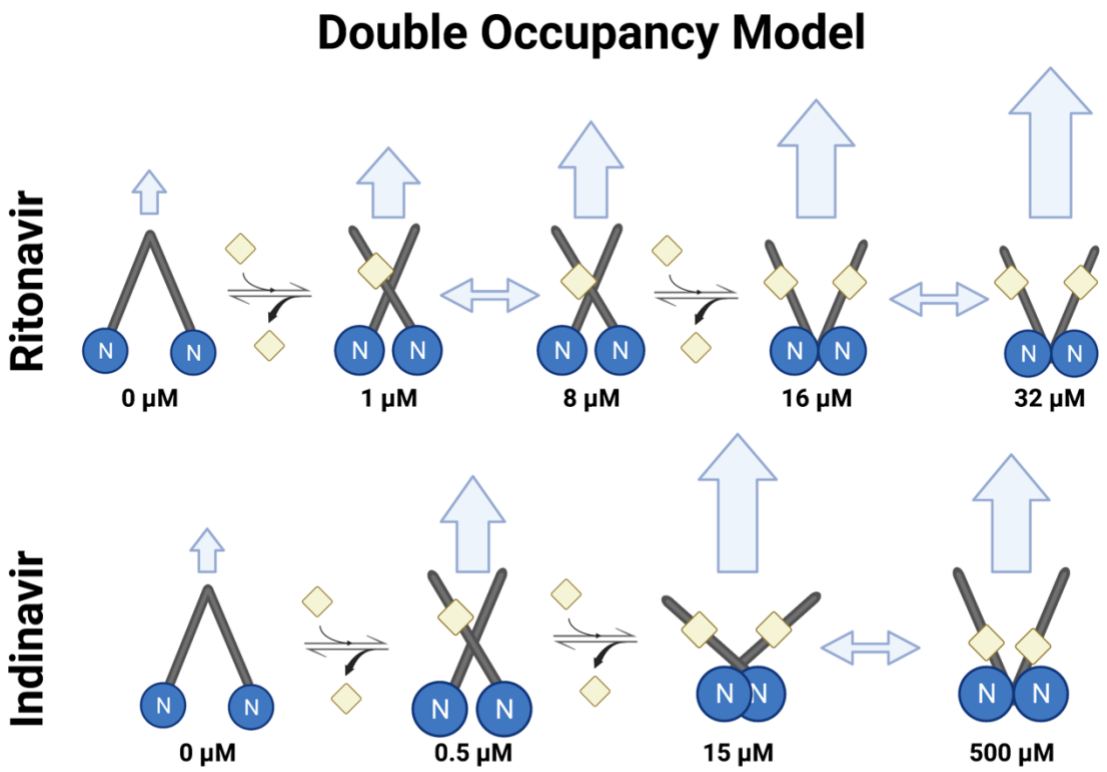

Figure 14 This represents the P-gp conformational state at each drug concentration. Crossed bars represent various conformational states of P-gp ranging from open, intermediate, and closed. Encircled N's represent NBD's. Diamonds represent drug substrate. The arrows above each state visually represent the ATPase activation around that concentration, based on the kinetics data.

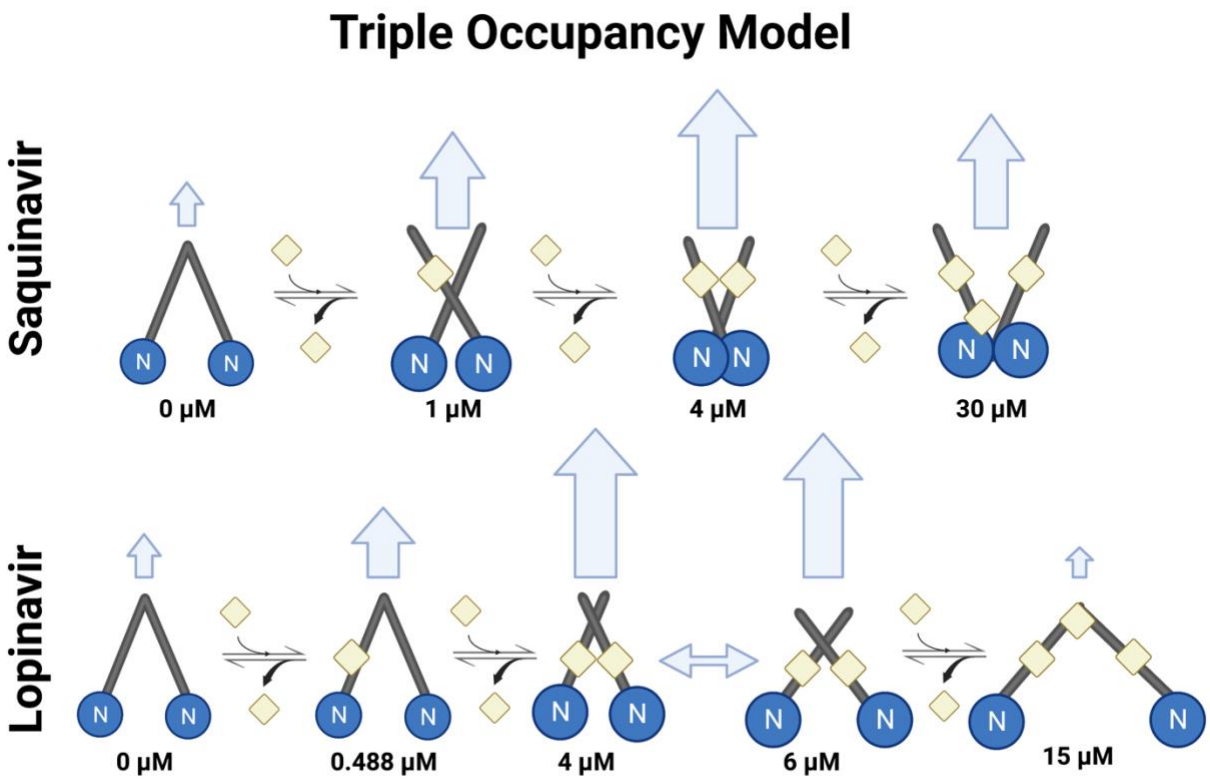

Figure 15 This represents the P-gp conformational state at each drug concentration. Crossed bars represent various conformational states of P-gp ranging from open, intermediate, and closed. Encircled N's represent NBD's. Diamonds represent drug substrate. The arrows above each state visually represent the ATPase activation around that concentration, based on the kinetics data.

These results provide unique insight into how four specific HIV PI drugs interact with P-gp. One of the most surprising finds was the three-phase ATPase kinetics exhibited by 2 of the drugs, indicating the existence of 3 potential binding sites – one of which is inhibitory. While this model points to the idea that increasing the drug concentration for PI's that follow the triple occupancy model can overcome P-gp's inhibitory effects, this might not be a practical solution in the clinic. First generation protease inhibitors already come with significant side effects, which are exacerbated by the higher oral dosages required due to their extensive first-pass metabolism and overall poor bioavailability. Because these drugs experience nonlinear patterns of absorption and subsequent excretion, which is caused by a myriad of confounding physiological factors such as complex CYP3A interactions, healthcare providers

must be careful to consider the many layers that contribute to the pharmacokinetic behavior of these drugs in clinical application.

The triple occupancy model of PI drug is not something to be applied in the clinic, but rather serves as a starting point from which to begin untangling the layers of mystery that confound our understanding of how PI's work so well as both substrate and inhibitor. Future work involving the aforementioned transport assay along with atomic force microscopy (AFM) could help us dig deeper down this path. These are techniques that are beyond the current everyday scope of this lab, but may be accessible to us in the near future. These results ultimately provide a model for deducing the behavior of first-generation PI drug binding with P-gp based on the kinetics of ATPase activation. Due to the similarities in their peptide-like structure, it is possible that this model can be applicable to all the first-generation HIV PI drugs. Future work could take this concept a step further and conduct these experiments with human P-gp to see whether a similar model could be deduced. Whether the models are similar or not, this could shed new light on how the structural differences between mouse and human P-gp affect their binding to substrates.

The models put forth from in this research aren't exhaustive. Future work should include more HIV PI drugs to see if they follow this line of behavior. It should also involve more structure analysis of the side groups beyond the peptidomimetic structure of these drugs (as highlighted in Figure 3). This could provide a deeper understanding of why they behave differently in terms of P-gp interactions.

A recent breakthrough was published that described Trojan horse prodrug therapies utilizing HIV protease inhibitors as asymmetric dimers, allowing them to bypass the limiting effects of the blood-brain barrier (Agrawal et al., 2020). Perhaps it will take some combination of P-gp modulation, out-of-the-box innovations like Trojan horse prodrug therapy, and thorough knowledge of which PI drugs follow the triple occupancy model of inhibition and which ones follow the double occupancy model of activation, to bring us within reach of overcoming the obstacles laid out by P-gp and sanctuary sites.

References

21-226_Kaletra_prntlbl.pdf. (2000). FDA. https://www.accessdata.fda.gov/drugsatfda_docs/nda/2000/21-226_Kaletra_prntlbl.pdf

20628ap_s007.pdf. (1997). FDA. https://www.accessdata.fda.gov/drugsatfda_docs/nda/97/20628ap_s007.pdf

020628s43-021785s19lbl.pdf. (2015). FDA. https://www.accessdata.fda.gov/drugsatfda_docs/label/2015/020628s43-021785s19lbl.pdf

020685s078lbl.pdf. (2016). FDA. https://www.accessdata.fda.gov/drugsatfda_docs/label/2016/020685s078lbl.pdf

209512lbl.pdf. (2017). FDA. https://www.accessdata.fda.gov/drugsatfda_docs/label/2017/209512lbl.pdf

Agrawal, N., Rowe, J., Lan, J., Yu, Q., Hrycyna, C. A., & Chmielewski, J. (2020). Potential Tools for Eradicating HIV Reservoirs in the Brain: Development of Trojan Horse Prodrugs for the Inhibition of P-Glycoprotein with Anti-HIV-1 Activity. *Journal of Medicinal Chemistry*, *63*(5), 2131–2138. https://doi.org/10.1021/acs.jmedchem.9b00779

Aller Stephen G., Yu Jodie, Ward Andrew, Weng Yue, Chittaboina Srinivas, Zhuo Rupeng, Harrell Patina M., Trinh Yenphuong T., Zhang Qinghai, Urbatsch Ina L., & Chang Geoffrey. (2009). Structure of P-Glycoprotein Reveals a Molecular Basis for Poly-Specific Drug Binding. *Science*, *323*(5922), 1718–1722. https://doi.org/10.1126/science.1168750

Barré-Sinoussi, F., Chermann, J. C., Rey, F., Nugeyre, M. T., Chamaret, S., Gruest, J., Dauguet, C., Axler-Blin, C., Vézinet-Brun, F., Rouzioux, C., Rozenbaum, W., & Montagnier, L. (1983). Isolation of a T-Lymphotropic Retrovirus from a Patient at Risk for Acquired Immune Deficiency Syndrome (AIDS). *Science*, *220*(4599), 868–871. https://doi.org/10.1126/science.6189183

Becker, S. (2018, November 28). Why the HIV epidemic is not over. *World Health Organization - Spotlight*. https://www.who.int/news-room/spotlight/why-the-hiv-epidemic-is-not-over

Bierman, W. F. W., Scheffer, G. L., Schoonderwoerd, A., Jansen, G., van Agtmael, M. A., Danner, S. A., & Scheper, R. J. (2010). Protease inhibitors atazanavir, lopinavir and ritonavir are potent blockers, but poor substrates, of ABC transporters in a broad panel of ABC transporter-overexpressing cell lines. *Journal of Antimicrobial Chemotherapy*, *65*(8), 1672–1680. https://doi.org/10.1093/jac/dkq209

BROOKS, T. A., KENNEDY, D. R., GRUOL, D. J., OJIMA, I., BAER, M. R., & BERNACKI, R. J. (2004). Structure-activity Analysis of Taxane-based Broad-spectrum Multidrug Resistance Modulators. *Anticancer Research*, *24*(2A), 409.

Calabrese, E. J. (2008). P-Glycoprotein Efflux Transporter Activity Often Displays Biphasic Dose-Response Relationships. *Critical Reviews in Toxicology*, *38*(5), 473–487. https://doi.org/10.1080/10408440802004049

Cerveny, L., Ptackova, Z., Durisova, M., & Staud, F. (2018). Interactions of protease inhibitors atazanavir and ritonavir with ABCB1, ABCG2, and ABCC2 transporters: Effect on transplacental disposition in rats. *Reproductive Toxicology*, *79*, 57–65. https://doi.org/10.1016/j.reprotox.2018.05.008

Chifflet, S., Torriglia, A., Chiesa, R., & Tolosa, S. (1988). A method for the determination of inorganic phosphate in the presence of labile organic phosphate and high concentrations of protein: Application to lens ATPases. *Analytical Biochemistry*, *168*(1), 1–4. https://doi.org/10.1016/0003-2697(88)90002-4

Choi, Y. H., & Yu, A.-M. (2014). ABC transporters in multidrug resistance and pharmacokinetics, and strategies for drug development. *Current Pharmaceutical Design*, *20*(5), 793–807. https://doi.org/10.2174/13816128200514021416521 2

Crommentuyn, K. M. L., Kappelhoff, B. S., Mulder, J. W., Mairuhu, A. T. A., van Gorp, E. C. M., Meenhorst, P. L., Huitema, A. D. R., & Beijnen, J. H. (2005). Population pharmacokinetics of lopinavir in combination with ritonavir in HIV-1-infected patients. *British Journal of Clinical Pharmacology*, *60*(4), 378–389. PubMed. https://doi.org/10.1111/j.1365-2125.2005.02455.x

Eagling, V. A., Back, D. J., & Barry, M. G. (1997). Differential inhibition of cytochrome P450 isoforms by the protease inhibitors, ritonavir, saquinavir and indinavir. *British Journal of Clinical Pharmacology*, *44*(2), 190–194. https://doi.org/10.1046/j.1365-2125.1997.00644.x

Eckford, P. D. W., & Sharom, F. J. (2008). Interaction of the P-glycoprotein multidrug efflux pump with cholesterol: Effects on ATPase activity, drug binding and transport. *Biochemistry*, *47*(51), 13686–13698. https://doi.org/10.1021/bi801409r

Esser, L., Zhou, F., Pluchino, K. M., Shiloach, J., Ma, J., Tang, W.-K., Gutierrez, C., Zhang, A., Shukla, S., & Madigan, J. P. (2016). Structures of the multidrug transporter P-glycoprotein reveal asymmetric ATP binding and the mechanism of polyspecificity. *Journal of Biological Chemistry*, *292*(2), 446–461. https://doi.org/10.1074/jbc.M116.755884

Frank, G. A., Shukla, S., Rao, P., Borgnia, M. J., Bartesaghi, A., Merk, A., Mobin, A., Esser, L., Earl, L. A., Gottesman, M. M., Xia, D., Ambudkar, S. V., & Subramaniam, S. (2016). Cryo-EM Analysis of the Conformational Landscape of Human P-glycoprotein (ABCB1) During its Catalytic Cycle. *Molecular Pharmacology*, *90*(1), 35. https://doi.org/10.1124/mol.116.104190

Gallo, R. C., Sarin, P. S., Gelmann, E. P., Robert-Guroff, M., Richardson, E., Kalyanaraman, V. S., Mann, D., Sidhu, G. D., Stahl, R. E., Zolla-Pazner, S., Leibowitch, J., & Popovic, M. (1983). Isolation of Human T-Cell Leukemia Virus in Acquired Immune Deficiency Syndrome (AIDS). *Science*, *220*(4599), 865–867. https://doi.org/10.1126/science.6601823

Ghosh, A. K., Dawson, Z. L., & Mitsuya, H. (2007). Darunavir, a conceptually new HIV-1 protease inhibitor for the treatment of drug-resistant HIV. *Bioorganic & Medicinal Chemistry*, *15*(24), 7576–7580. https://doi.org/10.1016/j.bmc.2007.09.010

Ghosh, A. K., Osswald, H. L., & Prato, G. (2016). Recent Progress in the Development of HIV-1 Protease Inhibitors for the Treatment of HIV/AIDS. *Journal of Medicinal Chemistry*, *59*(11), 5172–5208. https://doi.org/10.1021/acs.jmedchem.5b01697

Gibbs, M. E., Wilt, L. A., Ledwitch, K. V., & Roberts, A. G. (2018). A conformationally-gated model of methadone and loperamide transport by P-glycoprotein. *Journal of Pharmaceutical Sciences*. https://doi.org/10.1016/j.xphs.2018.02.019

Graves M C, Lim J J, Heimer E P, & Kramer R A. (1988). An 11-kDa form of human immunodeficiency virus protease expressed in Escherichia coli is sufficient for enzymatic activity. *Proceedings of the National Academy of Sciences*, *85*(8), 2449–2453. https://doi.org/10.1073/pnas.85.8.2449

Griffin, L., Annaert, P., & Brouwer, K. (2011). Influence of Drug Transport Proteins on Pharmacokinetics and Drug Interactions of HIV Protease Inhibitors. *Journal of Pharmaceutical Sciences*, *100*(9), 3636–3654. https://doi.org/10.1002/jps.22655

Hamdoun, A., Hellmich, U. A., Szakacs, G., & Kuchler, K. (2021). The incredible diversity of structures and functions of ABC transporters. *FEBS Letters*, *595*(6), 671–674. https://doi.org/10.1002/1873-3468.14061

Hayes, R. (2021, November). Life expectancy for people living with HIV. *Treatment Outcomes & Life Expectancy*. https://www.aidsmap.com/about-hiv/life-expectancy-people-living-hiv

Highleyman, L. (2022, February 16). *New York woman is free of HIV 14 months after stem cell transplant*. Aidsmap. https://www.aidsmap.com/news/feb-2022/new-york-woman-free-hiv-14-months-after-stem-cell-transplant

Hsu, A., Granneman, G. R., & Bertz, R. J. (1998). Ritonavir. *Clinical Pharmacokinetics*, *35*(4), 275–291. https://doi.org/10.2165/00003088-199835040-00002

Indinavir PK Fact Sheet. (2016). University of Liverpool. https://liverpool-hiv-hep.s3.amazonaws.com/fact_sheets/pdfs/000/000/082/original/HIV_FactSheet_IDV_2016_Mar.pdf?1458129926

Jain, S., Grandits, M., & Ecker, G. F. (2018). Interspecies comparison of putative ligand binding sites of human, rat and mouse P-glycoprotein. *European Journal of Pharmaceutical Sciences : Official Journal of the European Federation for Pharmaceutical Sciences*, *122*, 134–143. PubMed. https://doi.org/10.1016/j.ejps.2018.06.022

Janneh, O., Jones, E., Chandler, B., Owen, A., & Khoo, S. H. (2007). Inhibition of P-glycoprotein and multidrug resistance-associated proteins modulates the intracellular concentration of lopinavir in cultured CD4 T cells and primary human lymphocytes. *Journal of Antimicrobial Chemotherapy*, *60*(5), 987–993. https://doi.org/10.1093/jac/dkm353

Josephson, F. (2010). Drug–drug interactions in the treatment of HIV infection: Focus on pharmacokinetic enhancement through CYP3A inhibition. *Journal of Internal Medicine*, *268*(6), 530–539. https://doi.org/10.1111/j.1365-2796.2010.02301.x

Kim, R. B., Fromm, M. F., Wandel, C., Leake, B., Wood, A. J., Roden, D. M., & Wilkinson, G. R. (1998). The drug transporter P-glycoprotein limits oral absorption and brain entry of HIV-1 protease inhibitors. *The Journal of Clinical Investigation*, *101*(2), 289–294. https://doi.org/10.1172/JCI1269

Kim Youngjin & Chen Jue. (2018). Molecular structure of human P-glycoprotein in the ATP-bound, outward-facing conformation. *Science*, *359*(6378), 915–919. https://doi.org/10.1126/science.aar7389

Kodan, A., Futamata, R., Kimura, Y., Kioka, N., Nakatsu, T., Kato, H., & Ueda, K. (2021). ABCB1/MDR1/P-gp employs an ATP-dependent twist-and-squeeze mechanism to export hydrophobic drugs. *FEBS Letters*, *595*(6), 707—716. https://doi.org/10.1002/1873-3468.14018

Kumar, M., Mandal, K., Blakeley, M. P., Wymore, T., Kent, S. B. H., Louis, J. M., Das, A., & Kovalevsky, A. (2020). Visualizing Tetrahedral Oxyanion Bound in HIV-1 Protease Using Neutrons: Implications for the Catalytic Mechanism and Drug Design. *ACS Omega*, *5*(20), 11605–11617. https://doi.org/10.1021/acsomega.0c00835

Lakowicz, J. (2006). Principles of Fluorescence Spectroscopy. In *Principles of Fluorescent Spectroscopy, 3rd Edn* (Vol. 1). https://doi.org/10.1007/978-0-387-46312-4

Ledwitch, K. V., Gibbs, M. E., Barnes, R. W., & Roberts, A. G. (2016). Cooperativity between verapamil and ATP bound to the efflux transporter P-glycoprotein. *Biochemical Pharmacology*, *118*, 96–108. https://doi.org/10.1016/j.bcp.2016.08.013

Ledwitch, K. V., & Roberts, A. G. (2017). Cardiovascular ion channel inhibitor drug-drug interactions with P-glycoprotein. *The AAPS Journal*, *19*(2), 409–420. https://doi.org/10.1208/s12248-016-0023-y

Lerner-Marmarosh, N., Gimi, K., Urbatsch, I. L., Gros, P., & Senior, A. E. (1999). Large Scale Purification of Detergent-soluble P-glycoprotein fromPichia pastoris Cells and Characterization of Nucleotide Binding Properties of Wild-type, Walker A, and Walker B Mutant Proteins *. *Journal of Biological Chemistry*, *274*(49), 34711–34718. https://doi.org/10.1074/jbc.274.49.34711

Lledó-García, R., Nácher, A., Prats-García, L., Casabó, V. G., & Merino-Sanjuán, M. (2007). Bioavailability and Pharmacokinetic Model for Ritonavir in the Rat. *Journal of Pharmaceutical Sciences*, *96*(3), 633–643. https://doi.org/10.1002/jps.20683

Loo, T. W., Bartlett, M. C., Detty, M. R., & Clarke, D. M. (2012). The ATPase Activity of the P-glycoprotein Drug Pump Is Highly Activated When the N-terminal and Central Regions of the Nucleotide-

binding Domains Are Linked Closely Together *. *Journal of Biological Chemistry*, *287*(32), 26806–26816. https://doi.org/10.1074/jbc.M112.376202

Loo, T. W., & Clarke, D. M. (2016). P-glycoprotein ATPase activity requires lipids to activate a switch at the first transmission interface. *Biochemical and Biophysical Research Communications*, *472*(2), 379–383. https://doi.org/10.1016/j.bbrc.2016.02.124

Lv, Z., Chu, Y., & Wang, Y. (2015). HIV protease inhibitors: A review of molecular selectivity and toxicity. *HIV AIDS (Auckl)*, *7*, 95–104. https://doi.org/10.2147/HIV.S79956

Omeragic, A., Kayode, O., Hoque, M. T., & Bendayan, R. (2020). Potential pharmacological approaches for the treatment of HIV-1 associated neurocognitive disorders. *Fluids and Barriers of the CNS*, *17*(1), 42. https://doi.org/10.1186/s12987-020-00204-5

Perloff, M. D., Von Moltke, L. L., Marchand, J. E., & Greenblatt, D. J. (2001). Ritonavir induces P-glycoprotein expression, multidrug resistance-associated protein (MRP1) expression, and drug transporter-mediated activity in a human intestinal cell line. *Journal of Pharmaceutical Sciences*, *90*(11), 1829–1837. https://doi.org/10.1002/jps.1133

Robillard, K. R., Chan, G. N. Y., Zhang, G., la Porte, C., Cameron, W., & Bendayan, R. (2014). Role of P-glycoprotein in the distribution of the HIV protease inhibitor atazanavir in the brain and male genital tract. *Antimicrobial Agents and Chemotherapy*, *58*(3), 1713–1722. PubMed. https://doi.org/10.1128/AAC.02031-13

Rothnie, A., Theron, D., Soceneantu, L., Martin, C., Traikia, M., Berridge, G., Higgins, C. F., Devaux, P. F., & Callaghan, R. (2001). The importance of cholesterol in maintenance of P-glycoprotein activity and its membrane perturbing influence. *Eur Biophys J*, *30*(6), 430–442.

Storch, C. H., Theile, D., Lindenmaier, H., Haefeli, W. E., & Weiss, J. (2007). Comparison of the inhibitory activity of anti-HIV drugs on P-glycoprotein. *Biochemical Pharmacology*, *73*(10), 1573–1581. https://doi.org/10.1016/j.bcp.2007.01.027

Tang, M. W., & Shafer, R. W. (2012). HIV-1 Antiretroviral Resistance. *Drugs*, *72*(9), e1–e25. https://doi.org/10.2165/11633630-000000000-00000

UNAIDS Global AIDS Update 2022. (2022). UNAIDS. https://indanger.unaids.org

Urbatsch, I. L., Sankaran, B., Bhagat, S., & Senior, A. E. (1995). Both P-glycoprotein Nucleotide-binding Sites Are Catalytically Active (*). *Journal of Biological Chemistry*, *270*(45), 26956–26961. https://doi.org/10.1074/jbc.270.45.26956

van der Sandt, I. C. J., Vos, C. M. P., Nabulsi, L., Blom-Roosemalen, M. C. M., Voorwinden, H. H., de Boer, A. G., & Breimer, D. D. (2001). Assessment of active transport of HIV protease inhibitors in various cell lines and the in vitro blood–brain barrier. *AIDS*, *15*(4). https://journals.lww.com/aidsonline/Fulltext/2001/03090/Assessment_of_active_transport_of_HIV_protease.7.aspx

Vasiliou, V., Vasiliou, K., & Nebert, D. W. (2009). Human ATP-binding cassette (ABC) transporter family. *Human Genomics*, *3*(3), 281. https://doi.org/10.1186/1479-7364-3-3-281

Washington, C. B., Wiltshire, H. R., Man, M., Moy, T., Harris, S. R., Worth, E., Weigl, P., Liang, Z., Hall, D., Marriott, L., & Blaschke, T. F. (2000). The Disposition of Saquinavir in Normal and P-glycoprotein Deficient Mice, Rats, and in Cultured Cells. *Drug Metabolism and Disposition*, *28*(9), 1058.

Weber, I. T., & Agniswamy, J. (2009). HIV-1 Protease: Structural Perspectives on Drug Resistance. *Viruses*, *1*(3), 1110–1136. PubMed. https://doi.org/10.3390/v1031110

Yamazaki, M., Neway, W. E., Ohe, T., Chen, I.-W., Rowe, J. F., Hochman, J. H., Chiba, M., & Lin, J. H. (2001). In Vitro Substrate Identification Studies for P-glycoprotein-Mediated Transport: Species Difference and Predictability of in Vivo Results. *Journal of Pharmacology and Experimental Therapeutics*, *296*(3), 723–735.

Zastre, J. A., Chan, G. N. Y., Ronaldson, P. T., Ramaswamy, M., Couraud, P. O., Romero, I. A., Weksler, B., Bendayan, M., & Bendayan, R. (2009). Up-regulation of P-glycoprotein by HIV protease inhibitors

in a human brain microvessel endothelial cell line. *Journal of Neuroscience Research*, *87*(4), 1023–1036. https://doi.org/10.1002/jnr.21898

Zolnerciks, J. K., Booth-Genthe, C. L., Gupta, A., Harris, J., & Unadkat, J. D. (2011). Substrate- and Species-dependent Inhibition of P-glycoprotein-mediated Transport: Implications for Predicting in vivo Drug Interactions. *Journal of Pharmaceutical Sciences*, *100*(8), 3055–3061. https://doi.org/10.1002/jps.22566

Zsila, F. (2007). Overlapping ligand specificity of P-glycoprotein and serum alpha(1)-acid glycoprotein: Evidences and potential implications. *Curr Drug Metab*, *8*(6), 563–593.